Fall 2017

Yeast Dynamin and Ypt6 Converge on the GARP for Endosome-to-Golgi Trafficking

Pelin Makaraci
Missouri State University, Makaraci292@live.missouristate.edu

YEAST DYNAMIN AND YPT6 CONVERGE ON THE GARP FOR ENDOSOME-TO-GOLGI TRAFFICKING

A Masters Thesis

Presented to

The Graduate College of

Missouri State University

In Partial Fulfillment

Of the Requirements for the Degree

Master of Science, Biology

By

Pelin Makaraci

December 2017

YEAST DYNAMIN AND YPT6 CONVERGE ON THE GARP FOR ENDOSOME-TO-GOLGI TRAFFICKING

Biology

Missouri State University, December 2017

Master of Science

Pelin Makaraci

ABSTRACT

Protein recycling is an important cellular process required for cell homeostasis. Results from prior studies demonstrated that Vps1, a dynamin homologue in yeast, is implicated in protein recycling from the endosome to the *trans*-Golgi Network (TGN). However, the function of Vps1 in relation to Ypt6, a master GTPase in the recycling pathway, remains unknown. The present study reveals that Vps1 physically interacts with Ypt6 if at least one of them is full-length. It was found that overexpression of full-length Vps1, but not GTP hydrolysis-defective Vps1 mutants, is sufficient to rescue abnormal phenotypes in membrane trafficking pathways provoked by loss of Ypt6 or Vps1. This suggests an essential role of GTP binding and hydrolysis for Vps1 function in the traffic pathway. A series of data from our functional analyses suggest that Ypt6 and Vps1 function parallely for endosome-to-TGN trafficking. Additionally, I identified two novel Vps1 binding partners, Vti1 and Snc2, which function for the endosome-derived vesicle fusion at the TGN, suggesting that Vps1 plays a novel role in later stages of the endosome-to-TGN traffic.

KEYWORDS: Ypt6, Vps1, GTPase, TGN, fusion, SNARE, GARP, yeast, intracellular trafficking

This abstract is approved as to form and content

_____

Kyoungtae Kim, PhD
Chairperson, Advisory Committee
Missouri State University

YEAST DYNAMIN AND YPT6 CONVERGE ON THE GARP FOR ENDOSOME-TO-GOLGI TRAFFICKING

By

Pelin Makaraci

A Masters Thesis
Submitted to the Graduate College
Of Missouri State University
In Partial Fulfillment of the Requirements
For the Degree of Master of Science, Biology

December 2017

Approved:

_____
Kyoungtae Kim, PhD

_____
Paul L. Durham, PhD

_____
Ryan Udan, PhD

_____
Julie Masterson, PhD: Dean, Graduate College

ACKNOWLEDGEMENTS

First of all, I would like to thank my committee chair, Dr. Kyoungtae Kim, for his support, patience, and enthusiasm. I have come a long way under his guidance, and I appreciate it sincerely. I also would like to thank my committee members Dr. Paul Durham and Dr. Ryan Udan for their valuable time and encouragement throughout my time at Missouri State University. Additionally, I would like to thank my friends and colleagues Sara Woodman, Shiva Kumar Gadila, Uma Saimani, Mariel Delgado Cruz, Chelsea Campbell, Bryan Bahn, Jared Smothers, Tanner Hoog, Samantha Fredrickson, Hyoeun McDermott, and John Short for always being there to help me out in any obstacle both in professional and personal life and becoming my second family in another country. Next, I would like to thank my family who has done anything and everything possible to send me to another country to complete my education and my dear friend Tim Kearns for his unconditional support. Finally, I would like to acknowledge the Biology Department, the Graduate College, and Lt. Wolter for their financial assistance.

I dedicate this thesis to my parents and my sister

TABLE OF CONTENTS

LIST OF TABLES

LIST OF FIGURES

INTRODUCTION

Recent Advances in Membrane Trafficking

The communication between membrane-bound organelles is crucial for cell homeostasis (Spang, 2016). Membrane components, such as lipids and proteins that are essential for cell vitality, are transported between membrane-bound compartments via intracellular trafficking (Spang, 2016). Though the morphology of membrane-bound organelles is well studied, the molecular mechanisms behind the trafficking between these compartments are not entirely understood. Advanced microscopic analyses have allowed researchers to characterize the novel function of proteins implicated in trafficking pathways (Miller et al., 2015). For example, the fluorescence resonance energy transfer (FRET) technology was adopted to examine the conformational change of dynamin polymers caused by a structural change occurring in the dynamin PH (Pleckstrin Homology) domain upon binding at the surface of the membrane (Mehrotra et al., 2014). Furthermore, the authors proposed that the structural change in the PH domain contribute negatively to the dynamin-mediated membrane scission process. Another advanced fluorescence microscopy technique is called the stimulated emission depletion (STED) technology, which was developed to overcome the fluorescence microscopy resolution limitation (~200 nm) (van Weering et al., 2010). STED uses two different laser beams, one of which is used to excite the fluorophore and the other laser beam for bleaching the vast majority of fluorophores on the plane of focus, leaving a minimal number of fluorescence probes to be detected, thereby drastically improving the resolution (Hanne et al., 2015). Recently, the two-color STED was exploited to visualize for the first time the

recycling pathway of neurotransmitter molecules carried by inner hair cell synaptic vesicles of 40 nm in size, for the very first time by labeling the synaptic vesicle with a novel probe called mCLING (membrane-binding fluorophore-cysteine-lysine-palmitoyl group) (Revelo et al., 2014).

Interestingly, the correlative light electron microscopy (CLEM) technique uses the labeling power of the fluorescence microscopy and the resolution power of transmission electron microscopy to characterize and visualize the dynamics of subcellular compartments (de Boer et al., 2015). For instance, the ultrastructure of the parasitophorous vacuole (PV) carrying *Toxoplasma gondii* was investigated with the CLEM technique, shedding some insights into the mechanism behind the Rab-mediated fusion of the nutrient vesicle with the PV present in the host cytoplasm (Ru et al., 2015). In this study, *T. gondii* infected Hela cells were subjected to fluorescence microscopy to identify nutrient-carrying vesicles marked by fluorophores, and then these positive target cells were fixed and sectioned to be visualized under the electron microscope (Ru et al., 2015). The imaging results uncovered that fluorescently tagged nutrient filled host vesicles were trapped by the PV and were taken up by a process similar to phagocytosis, providing new insights into *T. gondii's* intracellular behavior (Ru et al., 2015).

Significance of the Intracellular Trafficking

Dysfunction of the intracellular trafficking can lead to diseases such as Alzheimer's disease that is characterized by the accumulation of amyloid-β (Aβ) in neurons, due to hyperactivation or overproduction of β-site amyloid precursor protein cleaving enzyme 1 (BACE1) , which cleaves the amyloid precursor protein (APP) for the

production of Aβ (Wang et al., 2014b). Alternatively, it has been shown that defects in retrograde traffic, involving membrane trafficking from the endosome to the Golgi, are associated with Alzheimer's disease (Buggia-Prévot and Thinakaran, 2015). Under this condition, endocytosed BACE1 resides persistently at the late endosome and furthermore, its enzyme activity is triggered by the acidic pH of the environment, resulting in elevated production of Aβ in the lumen of the late endosome (Ye and Cai, 2014). The accumulated Aβ are secreted from the cells via a recycling pathway to promote the Alzheimer's pathological condition (Ye et al., 2017). Therefore, understanding not only the regulation of the BACE1 activity during retrograde trafficking in detail but also other molecular requirements involved in the endosome-to-Golgi retrograde trafficking could be essential to intervene in Aβ production relevant to Alzheimer's disease pathologies (Zhang and Song, 2013).

The following sections are dedicated to the discussion of the main events and key molecules required for retrograde trafficking pathways. The retrograde transport of proteins involves two major cellular organelles, the *trans*-Golgi network (TGN) and endosomes. Therefore, in the next section the structure and function of the TGN will be discussed, followed by in-depth discussion of the mechanism underlying the endosome-to-Golgi traffic pathway.

trans-Golgi Network is the Center of Biological Cargo Delivery

The Golgi apparatus, consisting of multiple layers of the saucer-like membrane called cisternae, functions as a key protein sorting and shipping station of cells (Osterrieder, 2012). In higher eukaryotic cells, the Golgi apparatus consists of a stack of

3-20 cisternae (Suda and Nakano, 2012). However, the budding yeast *Saccharomyces cerevisiae* displays a morphology of separately distributed Golgi cisternae throughout the cell (Suda and Nakano, 2012). In eukaryotic cells, rough endoplasmic reticulum (ER) is the synthesis site of ER resident and secretory proteins. Secretory proteins are packed in an ER-derived transport vesicle and delivered from the rough ER to the Golgi complex. The Golgi complex can be separated into five regions: *cis*-Golgi network (CGN), *cis*-, *medial*-, *trans*-Golgi, and *trans*-Golgi network (TGN) (Mart et al., 2013). The CGN, situated closest to the ER, is responsible for both receiving ER-derived transport vesicles and shipping ER resident proteins back to the ER (Ishii et al., 2016). The TGN is located on the opposite side of the CGN, towards the *trans*-Golgi, and is involved in the final stage of sorting, packing, and delivering of most of, if not all, secretory proteins to their destinations (Crevenna et al., 2016).

In an exocytic event, cargo-carrying transport vesicles derived from the TGN travel to the plasma membrane. Upon fusion of the vesicle with the plasma membrane, soluble cargoes are secreted out to the extracellular matrix, but for transmembrane proteins, the plasma membrane is their final destination. Many externally located proteins, including collagens and cytokines, are secreted out of the cell via a constitutively active secretion pathway (Malhotra and Erlmann, 2015). However, some specialized cells store soluble proteins or small molecules in secretory vesicles to release on demand, responding to the external signals, and this process is referred to as regulated secretion. For instance, pre-synaptic nerve cells harbor secretory vesicles with neurotransmitters. In the case of binding of a chemical messenger to its receptor at the nerve cell plasma membrane, these vesicles travel toward and fuse with the plasma

membrane to release neurotransmitters to the extracellular matrix (Valenzuela and Perez, 2015).

The lysosome is another last stop for the cargo-carrying vesicle emerging from the TGN. Upon delivery, the majority of the cargo are activated to function as hydrolases at the lysosome. For example, α-glucosidase, a lysosomal hydrolase, contains a mannose-6-phosphate (M6P) that serves as a molecular tag for proper sorting at the TGN upon interaction with a cation-independent M6P receptor (CI-M6PR) (Schuller et al., 2013). Upon arrival at the late endosome, α-glucosidase dissociates from the receptor due to an acidic environment established in the lumen of the late endosome (Coutinho et al., 2012). CI-M6PR is then retrieved back to the TGN for the next round of cargo delivery (Schuller et al., 2013). In the budding yeast *Saccharomyces cerevisiae* function to coordinate, two parallel traffic pathways function to coordinate the delivery of cargo destined for the vacuole. Vacuolar enzymes of carboxypeptidase Y (CPY) and carboxypeptidase S (CPS) are first delivered to the endosome and then to the vacuole. In contrast, alkaline phosphatase (ALP) is directly transported to the vacuole from the TGN (Feyder et al., 2015). In particular, a soluble protease CPY is sorted in the lumen of the TGN with the help of its receptor Vps10 and transported to the endosome where CPY is dissociated from the receptor (Feyder et al., 2015). Vps10 recycles back to the TGN via a retrograde trafficking pathway, whereas CPY-carrying endosomes fuse with the vacuole to release the cargo.

A Diverse Range of Cargo for the Endosome-to-Golgi Retrograde Pathway

Internalization of extracellular materials along with the plasma membrane receptors on the cell occurs via a process called endocytosis (Irannejad et al., 2014). Post-endocytosed vesicles undergo a homotypic fusion with one another to form the early or sorting endosome, which matures into the late endosome by recruiting more Rab7 GTPase (Rink et al., 2005; Hegedus et al., 2016). Endosomes act as a central hub for protein traffic coming from endocytic and biosynthetic pathways, and for outgoing traffic to the plasma membrane. The latter includes at least three different routes, a fast recycling that rapidly occurs between the early endosome and the plasma membrane, a slow recycling that involves recycling vesicles, and lastly the retrograde trafficking that requires Golgi involvement (Schindler et al., 2015). The outgoing traffic from the endosome to the Golgi, the retrograde pathway, will be discussed comprehensively in this section.

The endosome-to-Golgi retrograde pathway is a crucial step for some external cargoes such as pathogenic toxins, including Shiga toxin from *Shigella dysenteriae,* cholera toxin from *Vibrio cholerae*, and ricin toxin from *Ricinus communi*, to avoid toxin degradation and to maintain the pathogen's toxicity (Burd, 2011). For instance, Shiga toxin that consists of a catalytic subunit (StxA) and a receptor binding subunit (StxB) follows the retrograde trafficking towards the TGN and then eventually arrives at the ER (Mukhopadhyay and Linstedt, 2013). From there, the StxA subunit uses the retrotranslocation machine at the ER to be released into the cytosol, where it interferes with ribosome functions, causing cytotoxicity (Garcia-Castillo et al., 2015). In addition to the external cargo, at least three types of internal cargoes follow the endosome-to-TGN

retrograde pathway: 1) sorting receptors including Wntless, M6PRs, Vps10, and sortilin; 2) transmembrane proteins including but not limited to furin, BACE1, SNAREs, TGN38, and TGN46; and finally, 3) ion and glucose transporters (Harterink et al., 2011; Klinger et al., 2015b; Mirsafian et al., 2014). These cargoes appear to be delivered to the TGN from either the early or late endosome (Figure 1A).

Furin, cation-dependent M6PR (CD-M6PR), cation-independent M6PR (CI-M6PR), and Vps10 are known to travel from the late endosome to the TGN, whereas cargoes including Wntless, sortilin, TGN38, and BACE1 are shipped from the early endosome to the TGN (Figure 1A) (Hierro et al., 2015; Klinger et al., 2015). Regardless of where the cargo is loaded, a proper retrograde trafficking toward the TGN requires a selected group of proteins including adaptor proteins, coat proteins, and sorting nexins (SNX). For instance, furin binds AP-1 adaptor protein via its acidic cluster sorting motif with the help of PACS1 (phosphofurin acidic cluster sorting protein 1) (Scott et al., 2003), and the furin-loaded vesicle emerging from the late endosome is coated by clathrin triskelions (Burd and Cullen, 2014b). Additionally, it is clear that the regulation of the retrograde traffic of furin to the TGN requires SNX15, an SNX1 homolog (Barr et al., 2000; Phillips et al., 2001). The endosomal sorting and transport of furin to the TGN is shown to be Rab9 GTPase-dependent since siRNA-mediated Rab9 knockdown resulted in severe defects in furin trafficking toward the TGN (Chia et al., 2011).

Interestingly, Rab9 GTPase is also a critical regulatory factor in the late endosome-to-TGN retrograde pathway of M6PRs (Diaz-Salinas et al., 2014). However, one fundamental difference between furin and CD-M6PRs retrograde trafficking pathways is that TIP47 instead of AP-1 serves as an adaptor protein for CD-M6PRs by

specifically interacting with the cytosolic FW (phenylalanine/tryptophan) sequence of the CD-M6PRs (Figure 1B) (Diaz and Pfeffer, 1998; Sincock et al., 2003). Unlike CD-M6PRs, CI-M6PRs do not contain this specific sequence motif. However, a competition binding experiment revealed that TIP47 interaction with CI-M6PR does occur via a membrane-proximal portion (48-75 amino acid residue) of the cytoplasmic domain of CI-M6PR (Orsel et al., 2000).

Another cargo that travels from the late endosome to the TGN is Vps10, a CI-M6PR equivalent in yeast. Remarkably, a study using immunoprecipitation and genetic complementation methods in yeast cells revealed that the Vps10 retrograde trafficking requires another coat protein complex called retromer, consisting of two subcomplexes: a cargo-selection subcomplex and a membrane-binding subcomplex (Trousdale, 2017). The former is a trimer of Vps35, Vps29, and Vps26, and the latter is a dimer of Vps5 and Vps17 (Figure 1B) (Horazdovsky et al., 1997; Seaman et al., 1998). The yeast cargo-selection subcomplex is conserved in mammalian systems (Swarbrick et al., 2011), and the mammalian sorting nexins of SNX1, SNX2, SNX5, and SNX6 are reported to be interchangeable equivalents of yeast Vps5 and Vps17 (Koumandou et al., 2011).

It is still debatable which retromer subcomplex is recruited first to endosomes, but based on to the findings of an RNA interference study the recruitment of these two retromer subcomplexes does not rely on each other (Seaman, 2012). The recruitment of the membrane-binding subcomplex depends both on BAR (Bin/Amphiphysin/Rvs) domains that recognize and bind the membrane curvature and PX (Phox homology) domains that interact with PI3P (Phosphatidylinositol 3-monophosphate) at endosomal membranes (Cullen and Korswagen, 2012). The cargo-selection subcomplex recruitment

largely depends on the interaction between Vps35 and the selective cargo (Harrison et al., 2014). Another known mechanism of the subcomplex recruitment to the endosomal membrane relies on the N-terminal conserved regions of Vps35 that interacts with Rab7 GTPase, a Rab GTPase highly concentrated at late endosomal membranes. However, low levels of Rab7 GTPase is detected at early endosomes membranes, indicating that Rab7 is present at all times at endosomes (Girard et al., 2014). Therefore, the retromer complex is implicated in cargo trafficking not only from the late endosome but also from the early endosome to the TGN (Guerra and Bucci, 2016).

One of the well-known cargoes of the retromer-mediated early endosome-to-TGN trafficking is BACE1 (Priya et al., 2015). According to an RNA interference assay result, the retrograde traffic of BACE1 requires SNX1/SNX2 dimeric subcomplex as well as SNX6 (Ye et al., 2017). The authors demonstrated that depletion of SNX6 leads to an accumulation of BACE1 at endosomes where it cleaves APP (amyloid precursor protein) to overproduce Aβ (Okada et al., 2010). Another group of researchers performed a similar RNA interference assay to discover the sorting nexin responsible for the APP trafficking from the early endosome to the TGN (Okada et al., 2010). It was shown that SNX17 depletion leads to overexpression of Aβ due to trafficking delay of APP from the early endosome to the TGN (Lee et al., 2008a). Human G protein-coupled receptor 177, commonly known as Wntless, is implicated in regulating the secretion of Wnt protein and is another cargo traveling from the early endosome to the TGN by the assistance of the retromer complex (Lee et al., 2008b). While investigating eight sorting nexins identified in the *Drosophila* genome, it was found that SNX3 is the essential molecule for the recycling of the Wntless trafficking from the early endosome to the TGN (Das et al.,

2012). This finding is supported by other researchers via deletion of SNX3, which resulted in Wntless accumulation at the early endosome and mistargeting of Wnt to the lysosome for degradation (Harterink et al., 2011). More examples of retromer cargoes can be found in the paper titled 'Retromer-Mediated Trafficking of Transmembrane Receptors and Transporters.' (Klinger et al., 2015).

It is clear that the variety of cargoes departing either the late or the early endosome creates the need for different sorting nexins, coat, and adaptor proteins. Once the sorting of the cargo is completed at the endosome, cargo-laden vesicles are pinched off of the endosome, moving towards the TGN.

Vesicle Fission at the Endosome and Movement towards the TGN

In the previous section, the processes of cargo recognition and sorting mediated by coat proteins, adaptors, and sorting nexins at endosomes were discussed. This section aims to provide up-to-date information on fission and movement of the endosome-derived vesicle destined for the TGN. Upon forming a cargo-laden vesicle at endosomes, numerous proteins, including but not limited to the WASH (Wiskott-Aldrich syndrome homolog) protein complex (consisting of Fam21, WASH1, CCDC53, SWIP, and strumpellin), Arp2/3 protein complex, and dynamin are recruited to endosomes for the vesicle fission (Figure 1C) (Klinger et al., 2015).

Vesicle fission. Apart from cargo recognition at endosomes, Vps35 is implicated in the recruitment of the WASH complex that regulates tubule dynamics at endosomes (Figure 1C) (Hunt and Stephens, 2011; Liu, 2017). Finding from recent studies showed that the interaction between the C-terminal end of Vps35 and the tail domain Fam21 (L-

F-(D/E) $_{3\text{-}10}$-L-F motif) of the WASH complex is required for targeting of the WASH complex to the endosome (McGough et al., 2014). Further details of this interaction were revealed while investigating a Vps35 point mutation that has been associated with Parkinson's disease symptoms. Increasing evidence suggests that the mutation of *vps35* ^{D620N} (aspartate to asparagine at the 620th amino acid) is commonly found in the genome of Parkinson's patients, and it is the only known pathological variant of Vps35 to date (Jia et al., 2012). The functional importance of this Vps35 mutation has been investigated by testing its interaction with Fam21. Expectedly, co-immunoprecipitation results showed that *vps35* ^{D620N} mutation abolished the interaction between *vps35* ^{D620N} and Fam21 and restricted the WASH complex recruitment to endosomes, significantly reducing the endosome-to-TGN trafficking of cargoes including CI-M6PRs (Vilarino-Guell et al., 2011; Zimprich et al., 2011). This research confirmed the functional significance of the retromer complex in endosome-to-TGN trafficking.

Upon recruitment to the endosome, WASH1, an actin nucleation-promoting factor (NPF), stimulates the Arp2/3 complex to generate cortical actin networks (Follett et al., 2014). A cortical actin binding protein called cortactin is another NPF that binds to the Arp2/3 complex to promote actin polymerization. Thus, it is possible that cortactin and the WASH complex cooperatively function to activate the same target, the Arp2/3 complex (Wang et al., 2014) (Figure 1C). In addition, the SH3 domain of cortactin plays an essential role in recruiting dynamin, a scission protein, to the endosome via the interaction between its SH3 domain and the PRD (proline-rich domain) of dynamin (Fritzsche et al., 2016). Noteworthy, the WASH complex also appears to be a major factor for the recruitment of dynamin (Zhu et al., 2005), because depletion of the WASH

complex has been shown to lead to the formation of long tubular structures at endosomes (Cosen-Binker and Kapus, 2006).

Dynamin in Action. The head (GTPase) domain of dynamin locates to its N-terminus, hydrolyzes GTP into GDP, and uses the energy produced by the hydrolysis event to drive membrane remodeling (Derivery et al., 2009). The GTPase domain is connected to a stalk domain that is involved in dynamin self-assembly to form a dynamin dimer, a preferable functional unit that is targeted to the neck of the emerging vesicle (Morlot and Roux, 2013). The authors of 'dynamin recruitment and membrane scission at the neck of a clathrin-coated pit' proposed that a dynamin polymer of 13-14 dimers forming a ring-like spiral around the neck of an emerging vesicle is sufficient enough to facilitate membrane fission (Cocucci et al., 2014). Regarding the fission activity of the dynamin polymer, two alternative models have been suggested: a two-stage model and a constricts/ratchet model (Cocucci et al., 2014). Similarily, both models support the notion that the GTPase activity of dynamin causes a constriction of the neck of an emerging vesicle (Figure 1C) (Smirnova et al., 1999; Chappie et al., 2011). Though dynamin's direct role on pinching off the emerging vesicle from the donor membrane has been controversial, it has been widely accepted that the constriction that dynamin collar creates around the neck of the vesicle tightens the elongated vesicle neck, leading to vesicle fission (Mattila et al., 2015).

The two-stage model involves dynamin assembly and disassembly that is highly coordinated with membrane constriction and scission, respectively. It proposes that dynamin assembly itself triggers membrane constriction, followed by GTP hydrolysis, by disassembly of dynamin polymer, and then by membrane scission (Antonny et al., 2016).

It was also proposed that every dynamin unit of the dynamin polymer participates in the GTP hydrolysis event. Considering that dynamin hydrolyzes a few GTPs per second, it is yet to be understood how all dynamin monomers stay GTP-bound until the dynamin polymer assembly is completed, which takes ~5-10 seconds.

On the other hand, the constrictase/ratchet model proposes that two distal ends of a dynamin polymer interact head-to-head (GTPase-to-GTPase) just like a zip tie, followed by a GTP-hydrolysis-mediated conformational change in the neck domain or bundle signal element (BSE) of dynamin heads (Bashkirov et al., 2008; Camley and Brown, 2011; Morlot et al., 2012). As a result of the BSE structural change, the dynamin molecules at the contact zone slide pass each other, thereby exerting a power stroke that causes membrane constriction, similar to myosin heads walking along actin filaments. Therefore, in this model, not every dynamin monomer contributes equally to membrane constriction.

Structurally, the PH domain, which allows dynamin-lipid interactions, is followed by a GED (GTPase Effector Domain) (Chappie et al., 2011; Sundborger et al., 2014). Multiple BSE domains are responsible for bringing the GTPase and the GED domains together to form the tertiary structure of dynamin (Faelber et al., 2011; Hegedus et al., 2016). The GED domain contains the PRD that is required for dynamin interactions with SH3-domain carrying proteins including but not limited to cortactin, amphiphysin, syndapin, and endophilin (Chappie and Dyda, 2013). Even though the GTPase domain is essential for the constriction related activities, mutations of the stalk or the PH domain of dynamin2 (a dynamin isoform) including L570H (570^{th} leucine to histamine), E368K/Q (368^{th} glutamic acid to lysine or glutamine), R369Q/W (369^{th} arginine to glutamine or

tryptophan), and R465W (465th arginine to tryptophan) are known to be associated with Charcot–Marie–Tooth neuropathy (CMT) and Centronuclear Myopathy (CNM) neurological disorder (Hill et al., 2001; Sundborger et al., 2014; Luo et al., 2016), emphasizing the functional importance of all dynamin domains.

Sorting Nexins Facilitate the Endosome-Derived Vesicle Movement towards the TGN. Dynamin-mediated vesicle fission is followed by the movement of the pinched-off vesicle towards the TGN, which is mediated by dynein and dynactin motor proteins that direct the vesicle movement on microtubules (Ryder et al., 2013). It has been shown that both retromer-dependent and independent vesicle movement toward the TGN is facilitated by sorting nexins (Figure 2A) (Chowdhury et al., 2015). The retromer-dependent endosomal cargo movement towards the TGN is proposed to be mediated by SNX6 binding to the p150^{Glued} domain of dynactin (Hunt et al., 2013). Moreover, it was shown that disruption of SNX6 binding with dynactin significantly reduces the endosome-to-TGN trafficking of CI-M6PR (Hong et al., 2009), supporting that SNX6 regulates the retromer-dependent vesicle movement of endosomal cargoes. Dynactin plays a role of a linker between the cargo and dynein, which allows dynein to tether the cargo to microtubules. Results from another study demonstrated that SNX8 correlates with retromer-independent endosomal cargo tubulation and export from endosomes, by coupling with dynein (van Weering et al., 2012). Cargo-linked dynein hydrolyzes ATP to generate force for the vesicle movement toward the minus end of microtubules to reach the TGN (Figure 2A) (Hong et al., 2009).

Dynamin and Dynamin-Like Proteins for Membrane Scission. Dynamin's scission role was first identified in a study of clathrin-mediated endocytosis (Llorente et

al., 1998). HeLa cells expressing GTP binding deficient dynamin mutants including K44A (lysine replaced with alanine) showed defects in clathrin-mediated endocytosis, manifested by the presence of elongated tubules at the plasma membrane (Llorente et al., 1998). In another study, K44A dynamin mutant was used to examine the efficiency of the retrograde pathway of ricin toxin (Damke et al., 1994). For this, expression of the dynamin mutant was induced by tetracycline right after ricin was internalized, and the trafficking of ricin toward the Golgi was examined with an electron microscope (Damke et al., 1994). Unexpectedly, in this dynamin mutant cell, the post-endocytosed ricin trafficking from the endosome to the Golgi was significantly impaired, supporting the hypothesis that dynamin is essential for the endosome-to-Golgi trafficking of ricin.

The dynamin-like proteins, such as the dynamin homologue in yeast called vacuolar sorting protein-1 (Vps1), are also associated with scission activity. For instance, cells expressing Vps1 I649K (isoleucine to lysine) mutant that is defective in self-assembly showed the formation of long endocytic tubules via the use of fluorescence and electron microscopy, which supports Vps1's role as a pinchase for endocytic vesicles (Mishra et al., 2011). It is noteworthy that during endocytosis the activation of Vps1 is regulated by its dynamic phosphorylation and dephosphorylation. Global phosphoproteome studies revealed that at least 4 amino acid)s of Vps1 are the targets for phosphorylation (Mishra et al., 2011). It has been reported that one of these residues, S599, is phosphorylated by Pho85, a cyclin-dependent kinase (Albuquerque et al., 2008; Swaney et al., 2013). Further, it was revealed that S599D (serine to aspartic acid) mutation, mimicking hyperphosphorylation, does not lead to any defects in non-endocytic functions such as CPY delivery to the Golgi, but it affects endocytic efficiency,

manifested by the formation of long invagination tubes (Smaczynska-de et al., 2015). Taken together, phosphorylation of the S599 residue is specific and critical for Vps1's endocytic activity. Moreover, Vps1 S599D mutant impedes the Vps1's binding to the yeast amphiphysin Rvs167, resulting in decreased efficiency of endocytic vesicles fission (Smaczynska-de et al., 2015). These data indicate that a dynamic phosphorylation-dephosphorization cycle of Vps1 is essential for a strong Vps1-Rvs167 interaction to facilitate proper endocytosis in the cell.

In addition to the plasma membrane, Vps1 localizes to a wide range of intracellular structures including peroxisomes, endosomes, vacuoles, and the Golgi (Smaczynska-de Rooij et al., 2016). Fluorescence and electron microscopic images showed that loss of Vps1 causes the formation of enlarged endosomes and severe defects in retrograde trafficking of Vps10, suggesting that Vps1 functions as a pinchase at endosomes (Williams and Kim, 2014; Goud Gadila et al., 2017; Saimani et al., 2017). Consistently, recent research demonstrated that double deletion mutation of Vps1 and a retromer complex subunit in *Saccharomyces cerevisiae* cells leads to more severe defects of Vps10 retrieval from the vacuole, compared with mutant cells with a single deletion of Vps1 or the retromer component (Trousdale, 2017). Although a yeast two-hybrid assay result from indicates that there is no physical interaction between Vps1 and any retromer subunits, the study provides evidence that Vps1 and the retromer complex cooperate for the retrieval of Vps10 from the vacuole. However, the precise mechanism of the cooperative nature of Vps1 and the retromer complex is unknown. Taken together, these data support Vps1's role in membrane scission at the endosome. However, the question of whether Vps1 acts as a pinchase at the TGN remains unanswered. Even though the

role of Vps1 at the TGN is yet to be described, the results of co-localizations assays using fluorescently tagged TGN markers clearly support the localization of Vps1 at the TGN (Arlt et al., 2015; Goud Gadila et al., 2017).

Involvement of Dynamin-Like Proteins in Membrane Fusion. Although the relevance of dynamin family members for the membrane fission has been well documented, a novel observation by Peters and his coworkers in which loss of Vps1 effects on vacuolar systems provided new insights into the function of dynamin-like proteins (Peters et al., 2004). It was observed that loss of Vps1 led to the formation of many small fragmented vacuoles, which is the most specific evidence of membrane fusion defects (Peters et al., 2004). This paper provided a new perspective that Vps1 may play a novel role in the homotypic fusion of vacuoles. Recently, lines of evidence showed that absence of Vps1 abolishes physical interactions between SNARE proteins (Vam3 and Nvy1), as well as the interaction of SNARE with tether (Vam3 and the HOPS complex), strengthening the notion that Vps1 plays a role in membrane fusion events (Kulkarni et al., 2014).

In addition, a collaborative nature between Vps1 and Vps51, a subunit of the GARP (Golgi-associated retrograde protein), has been shown (Saimani et al., 2017). In this study, the results of fluorescent microscopy indicate that the absence of Vps1 causes mistargeting of Vps51. Moreover, when the interaction between Vps1 and Vps51 is compromised, severe defects in the endosome-to-Golgi trafficking of Snc1 were observed, indicating that Vps1 is required for an efficient endosome-derived vesicle tethering at the Golgi (Saimani et al., 2017). It appears that Vps1 plays a role for late

processes of membrane fusion. However, the detailed mechanism of Vps1 recruitment to the Golgi and how it mediates the fusion process is not entirely understood.

Endosome-Derived Vesicle Tethering and Fusion at the TGN

Post-pinched off vesicles derived from the endosome carries a spectrum of transmembrane proteins including membrane cargo and SNAREs, as well as coat proteins and adaptors (Baker and Hughson, 2016). As a vesicle is approaching the TGN, it undergoes a rapid uncoating event in which coat proteins such as the retromer complex are dissociated from the vesicle (Trahey and Hay, 2010). Following the arrival at the TGN, cargo unloading requires three main steps including tethering, docking, and fusion (Figure 2B). First, tethering factors function in recognition of the incoming vesicle and loosely link it to the TGN membrane (Ma et al., 2016). Second, docking of the vesicle occurs by binding of a vesicle-SNARE (v-SNARE) with three TGN-SNAREs (t-SNAREs) (Chia and Gleeson, 2014). Finally, the interaction of SNAREs forms a 4-alpha-helix bundle called *trans*-SNARE complex, which strengthens the link between the vesicle and the TGN and overcomes the energy barrier that prevents two membranes from fusing (Seemann et al., 2000).

In general, tethering factors are separated into two groups, coiled-coil tethers and multisubunit tethering complexes (MTCs) (Brown et al., 2011). The coiled-coil tethers, including but not limited to p115, GM130, and Giantin, function at the Golgi to anchor Golgi or ER-derived vesicles (Murray et al., 2016). Another tethering factor called GCC185 has been shown to anchor endosome-derived vesicles to the TGN (Brunet and Sacher, 2014). EEA1 is implicated in docking and tethering of incoming vesicles to the

early endosome (Brunet and Sacher, 2014). The GARP, TRAPP (Transport Protein Particle) I/II, COG (Conserved Oligomeric Golgi), and HOPS complexes fall into the category of MTCs (Chia and Gleeson, 2014); The first three complexes function at the Golgi, whereas the last one mediates homotypic fusion of vacuolar membranes (Gillingham and Munro, 2016).

The focus of next section will be on the Golgi operating tethers including golgins, the GARP, COG and the TRAPPII complex. However, the detailed mechanisms of other tethering factors can be found elsewhere (Brown et al., 2011).

Golgi Localized Coiled-Coil Proteins. Golgi membranes host many long coiled-coil tethers that are often referred to as golgins (Reddy et al., 2006). For instance, a golgin called GCC185 has been identified at the TGN and to mediate heterotypic fusion of both the early and the late endosome-derived vesicles carrying cargoes including TGN38 or M6PR to the TGN (Reddy et al., 2006). In addition, observation of live cell video microscopy images revealed that GCC185 specifically captures Rab9-tagged vesicles (Cheung et al., 2015; Cheung and Pfeffer, 2016). Rab9 binding to GCC185 has been shown to facilitate a bubble-like structure in the middle of GCC185 to interact with the incoming vesicle to the TGN to pull it closer to TGN membranes (Figure 2B) (Bonifacino and Rojas, 2006). Even though the detailed mechanism of how GCC185 facilitates the membrane tethering needs to be further defined, results from a recent study support that GCC185 is not as rigid as it was previously thought but can bend and even collapse onto the Golgi membrane once it catches the incoming vesicle (Brown et al., 2011; Cheung et al., 2015; Cheung and Pfeffer, 2016). According to this collapse model, Rab9-carrying vesicles may be captured by the centrally located bubble at GCC185 to

facilitate the collapse onto the TGN surface. The energy required for the vesicle anchoring and pulling to the TGN is possibly facilitated by small GTPase of Rab6 and Arl1 that physically bind to the N-terminal of GCC185 (Puthenveedu and Linstedt, 2001; Radulescu et al., 2011). In addition to GTPases, GCC185 interacts with a protein named CLASPs (cytoplasmic linker associated proteins) and recruits them to the TGN (Efimov et al., 2007; Lin et al., 2011). CLASPs are responsible for microtubule formation and stabilization at the TGN (Efimov et al., 2007; Miller et al., 2009). CLASPs selectively play a role in the noncentrosomal microtubule nucleation at the TGN membranes by interacting with a plus-end tracking protein (+TIP) called cytoplasmic linker protein (CLIP). CLIPs are associated with the distal ends of microtubules to promote microtubule growth and vesicle delivery (Galjart, 2005; Grimaldi et al., 2014).

Besides serving as the anchor of an incoming vesicle, golgins play a critical role in the maintenance of the Golgi structure. Data from an antibody microinjection assay showed that knockdown of *cis*-Golgi golgin p115 dramatically disturbs the Golgi structure (Hirata et al., 2015). Previously, it was proposed that p115 cooperates with two other *cis*-Golgi located golgins, GM130 and Giantin, to maintain the Golgi structure. However, knockdown of neither GM130 nor Giantin negatively affected the Golgi structure. Therefore, these two proteins are required for incoming vesicle tethering but not essential for the Golgi structural maintenance. However, further investigation is required to test other potential roles of these golgins.

Multisubunit Tethering Complexes (MTCs). Among Golgi localized MTCs, the GARP anchors incoming vesicles for the recycling of membrane proteins from endosomes to the TGN (Abascal-Palacios et al., 2013). It has been shown that depletion

of subunits of the GARP abolishes the delivery of endosome-derived cargoes including Shiga toxin, TGN46, and CI-M6PRs to the TGN, supporting the notion that the GARP complex is required for the endosome-to-TGN trafficking (Pérez-Victoria et al., 2010).

The 4 subunits of the GARP complex, Vps52, Vps53, Vps54, and Ang2 (yeast Vps51 homologue), present in the cytosol until their recruitment to the TGN that is assisted by Rab6 (or yeast homologue Ypt6) (Perez-Victoria et al., 2008). The GARP complex interacts with a variety of SNAREs, acting as their upstream factor at the TGN (Fridmann-Sirkis et al., 2006; Abascal-Palacios et al., 2013). For instance, if the incoming vesicle is originated from the early endosome, Vps53/Vps54 dimer binds to the SNARE motif of syntaxin 6/syntaxin 16/VAMP4, which eventually creates a *trans*-SNARE complex with the participation of Vti1 (Figure 2B) (Perez-Victoria and Bonifacino, 2009). For the late endosome-derived vesicle tethering, the GARP complex assists the syntaxin 16/Vti1a/ syntaxin 10/VAMP3 *trans*-SNARE complex formation (Figure 2B) (Suda et al., 2013).

Similarly, yeast Vps51 interacts with Tlg1, a TGN t-SNARE, to ensure the vesicle tethering is followed by the docking/fusion stage (Figure 2C) (Furuta et al., 2007). This was supported by *VPS51* deletion experiment that resulted in a significant reduction of the *trans*-SNARE complex formation at the Golgi (Siniossoglou and Pelham, 2002). However, deletion of *VPS51* did not affect the tethering role of the GARP complex (Chen et al., 1992), indicating that the presence of three subunits of the GARP, namely Vps52, Vps53, and Vps54, is sufficient enough to promote the tethering, even in absence of Vps51. Taken together, it is clear that the GARP complex facilitates the endosome-

derived vesicle tethering/fusion at the TGN (Lees et al., 2010). Though, the question of how the GARP complex hooks the vesicles is not well understood.

The COG complex is another MTC, which contains eight subunits. In yeast, COG1-4 are categorized as essential core factors for viability, whereas COG5-8 as not essential. (Lees et al., 2010). Mammalian cells contain counterparts of yeast COG1, COG2, and COG7, while carrying homologues of other COG subunits (Scott et al., 2014). Even though the COG complex is shown to play a role in the retrograde trafficking of toxins including Shiga toxin (Climer et al., 2015), it is more likely that the COG complex mainly acts in the intra-Golgi trafficking pathways rather than endosomal cargo delivery to the TGN (Suvorova et al., 2002; Oka, 2004; Willett et al., 2014). Recently, it has been reported that mutations of *COG7* alter Golgi trafficking and lead to defects in glycosylation pathways (Smith and Lupashin, 2008). In support of this finding, genomic and physical interaction assays performed in yeast cells and revealed that the COG complex genetically and physically interacts with COPI and Ypt1, highlighting the tethering role of the COG complex as a connector of COPI-carrying vesicle at the cis-Golgi (Oka et al., 2004; Sohda et al., 2010). Also, in yeast, the COG complex has been shown to regulate the localization of both TGN-localized proteins and ER-originated cargo proteins (Thomas and Fromme, 2016).

Lastly, the TRAPPII complex consisting of ten subunits (Bet5, Tes20, Trs23, Trs31, Trs33, Trs85, Trs65, Trs120, Trs130, and Bet3) locates at the TGN, but its function is poorly understood (Lupashin and Sztul, 2005). In the light of new studies, it has been shown that TRAPPII recognizes COPI/II tagged vesicles and tethers them to Golgi membranes (Barrowman et al., 2010). Even though the exact mechanism behind

how the TRAPPII tethering occurs remains elusive, it has been proposed that in yeast cells Bet3 recruitment to the Golgi triggers other TRAPPII subunit recruitment (Barrowman et al., 2010).

SNAREs for Membrane Fusion. Tethering factors allow the incoming vesicle to loosely anchor to the TGN membrane loosely. Subsequent membrane docking and fusion steps require a transmembrane protein group called SNAREs (Krämer and Ungermann, 2011). SNAREs are often inserted into membranes via their C-terminally located transmembrane domain, whereas their N-terminal domain is located in the cytosol (Rizo and Xu, 2013). The cytosolic domain of SNAREs carries a conserved SNARE motif, which consists of heptad repeats of 60-70 amino acids and has the ability to form a coiled-coil structure (Wesolowski and Paumet, 2010). During membrane fusion, SNAREs are associated together to form a four-helical SNARE bundle (Elfrink et al., 2012). The core of this bundle is referred as the zero ionic layer (0-layer) (Fasshauer, 2003). In general, a v-SNARE presents an arginine (R) residue to form the 0-layer, whereas each of three t-SNAREs provides a glutamine (Q) residue (Liu et al., 2016). Therefore, v-SNAREs and t-SNAREs are often referred as R-SNAREs and Q-SNAREs, respectively. Q-SNAREs can be further classified as Qa, Qb, or Qc depending on their location in the four-helix bundle (Elfrink et al., 2012; Scheper and Hoozemans, 2015). Though a tight assembly of a *trans*-SNARE requires four different SNAREs (Figure 2B and C) (Alpadi et al., 2012), it was reported that synaptobrevin/syntaxin-1/ SNAP-25 are sufficient enough to form a *trans*-SNARE complex during the synaptic vesicle fusion with the plasma membrane since SNAP-25 presents two SNARE motifs instead of one (Halemani et al., 2010).

Membrane fusion requires energy to disrupt the lipid bilayer and finally to reorganize the curved membrane structures (Ungermann and Langosch, 2005). When the *trans*-SNARE complex is formed, t- and v-SNAREs are still located on the opposing membranes but slowly getting closer by the bundling of the SNARE motifs, which leads to the formation of a more stable and tighter *trans*-SNARE complex. Bundling of the SNAREs also results in the blockage of disassociation of the incoming vesicle from the TGN membrane (Hong and Lev, 2014). Moreover, it was proposed that bundling of SNAREs leads to a conformational change in *trans*-SNARE complexes, which creates a force on the transmembrane domains of SNAREs, leading to an unstable configuration of transmembrane domains. The conformation change in the transmembrane domain confers a driving force to overcome the energy barrier caused by the negative charges of phospholipid head groups of the lipid bilayers of the incoming vesicle and target membranes, allowing opposite membranes to fuse (Risselada and Grubmüller, 2012; Lou and Shin, 2016). Upon membrane fusion, SNAREs come together at the same membrane and form a *cis*-SNARE complex. The lipid reorganization occurs at the fusion pore upon membrane fusion for the mixing of the donor components to the acceptor compartment (Figure 2C). Finally, an adaptor protein called α-soluble NSF attachment protein (α-SNAP) disassembles the *cis*-SNARE complex, freeing the v-SNARE to be recycled back to the donor compartment (Fukasawa et al., 2013).

A large number of SNAREs are expressed in cells and shown to localize at particular membrane compartments, implying that specific pairing of SNAREs is needed for the specificity of the membrane fusion events. Recently, the classic paradigm that states that specific SNARE pairing is required for membrane fusion has been challenged.

Through immunoprecipitation assays it has been shown that SNAREs can interact with both non-cognate and cognate SNAREs with a similar affinity, if not greater, suggesting that SNARE-SNARE interactions are promiscuous (Südhof and Rizo, 2011). For instance, syntaxin6 has been shown to bind a series of SNAREs including, Vamp2, Vamp4, Vam7, Vamp8, SNAP25, and SNAP29 with a different affinity for different cell types examined, suggesting that syntaxin6 is involved in a variety of membrane fusion events (Wendler and Tooze, 2001). A study performed in PC12 cells showed that SNARE-SNARE interactions are much more specific in the cell than the ones observed *in vitro* reconstitution experiments, indicating that specific SNARE interactions are facilitated by other proteins, including the SM (Sec1/Munc18-like) proteins, suggesting that not every SNARE-SNARE interaction creates a functional *trans*-SNARE complex (Lerman et al., 2000; Liang et al., 2013). Munc18 has been shown to bind an α-helical SNARE domain of syntaxin1, leading to a closed conformation of syntaxin1 that is incapable of binding other SNAREs (Weninger et al., 2003). However, Munc13 interaction with syntaxin1 leads to the transition of the closed conformation of syntaxin1 into an open conformation, enabling the SNARE motif of syntaxin1 to interact with other SNAREs (Ma et al., 2011). Vps33, a HOPS tethering complex subunit, is another example of SM proteins that positively regulate SNAREs fusion activity. Vps33 has been shown to spontaneously bind to Nyv1 and Vam3 SNAREs to regulate the formation of the *trans*-SNARE complex for the homotypic fusion of vacuolar membranes (Baker et al., 2013). Surprisingly, Vps1 can be listed as another example of SNARE regulatory protein. Vps1 is determined to act as a linker between Vam3 and Nvy1 as well as Vam3

and the HOPS complex (Alpadi et al., 2013; Kulkarni et al., 2014), supporting the idea of fusion process requiring a complicated protein complex in addition to SNAREs.

Small GTPases Mediates Membrane Trafficking. Mammalian cells contain up to 70 types of Rab GTPases that uniquely localize in different components of the cell to regulate vesicular traffic (Wandinger-Ness and Zerial, 2014). Structural analysis has shown that a Rab protein is composed of a six-stranded β-sheet flanked by five α-helices that are common to all Ras superfamily members. COOH-terminal of Rabs has a hypervariable region that anchors the protein in cell membranes or cytoplasmic face of a vesicle and facilitated protein-protein interactions (Li et al., 2014). Additionally, C-terminal of Rabs contains CAAX boxes containing two cysteine residues that geranylgeranyl tails bind to regulate membrane insertion of Rabs (Lall et al., 2015). Another region of Rabs is the switch I and II that bind to γ phosphate of GTP (Stein et al., 2012).

In the cytoplasm, the GDP-bound Rab is associated with a GDP disassociation factor (GDI) to prevent the exchange of GDP for GTP (Oesterlin et al., 2012). However, a GDI-dissociation factor (GDF) has been suggested to disable this interaction and target Rab to the appropriate membrane. Upon nucleotide binding by a guanine nucleotide exchange factor (GEF), Rabs are activated and are delivered to their destination membranes by Rab escort proteins (REPs) (Barr and Lambright, 2010). Once Rab is no longer needed at the targeted membrane, a GTPase accelerating protein (GAP) binds to the membrane-bound Rab to help it hydrolyze GTP to GDP.

Members of Arl (Arf-like) and Rab GTPases bind to the GARP complex at the TGN membrane (Figure 2C) (Yang and Rosenwald, 2016). It was demonstrated that

overexpression of Rab6 stimulates the cargo delivery originated from endosomes to the TGN, thereby suggesting that Rab6 is the main regulator of the endosome-to-Golgi trafficking (Micaroni et al., 2013). In *S. cerevisiae*, GTP-bound Ypt6, the Rab6 homologue, shows genetic and physical interaction with Vps52 and, and GTP-bound Arl1 binds to the GARP complex through its Vps53 subunit. (Siniossoglou, 2005; Benjamin et al., 2011). Results from immunofluorescence microscopy studies indicate that depletion of Ypt6 leads to a reduction of the GARP complex recruitment to the TGN, whereas depletion of Arl1 does not affect the GARP complex localization to the TGN (Siniossoglou and Pelham, 2001; Panic et al., 2003; Bonifacino and Hierro, 2011). Thus, it is suggested that Arl1 might regulate other functions of the GARP complex instead of recruitment. Though the detailed mechanism of GARP recruitment to the TGN requires further investigations, it is proposed that the interaction of Ypt6 and Vps52 facilitates a triggering effect on the assembly of the GARP complex to the tethering site at the TGN (Hutagalung and Novick, 2011).

Concluding Remarks

For the last three decades, evidence from lines of studies has begun to reveal the main steps of the retrograde trafficking pathway and important factors regulating the traffic. It has been well established that dysregulation of these factors is tied to a wide range of human disorders. A clear understanding of the mechanisms behind the phenotypic defects or disease conditions provoked by dysregulation of these factors has provided new ideas on identifying and developing novel therapeutic targets to mitigate these pathological conditions. Though a general mechanism behind the endosome-to-

TGN trafficking has been somewhat revealed, the existing data is insufficient to draw conclusions on how different classes of tethering molecules or complexes, including golgin, GARP, and COG, catch specific cargo-carrying transport vesicles arriving at the TGN. Emerging evidence suggests that the interaction between a tether and a transport vesicle stimulates a conformational change of the tether, which brings the vesicle into close proximity to the TGN. However, the clear source of the energy that drives the conformational change in the tether has not been well documented. Furthermore, the question of whether there exists any functional cooperation between different tethers is of interest. Tethers appear to act as a multi-adhesive factor at the surface of the target membrane, and their interaction network involves a number of GTPases, including Arl1. Nevertheless, the physiological significance of the interaction awaits further exploration. An interesting paradigm change in the field involves a functional connection between the tether and the SNARE, possibly creating a multipartite protein complex, which is supported by numerous biochemical investigations. Importantly, the molecular mechanism of dynamic connection between them and the spatiotemporal assembly of the complex will likely to help us understand the last step of the endosome-to-TGN traffic. Dynamin family proteins play multiple roles including fission and fusion of membranes. Clearly, these dynamic proteins are in the big assembled structure residing at the TGN to facilitate tethering/fusion step. Yet, their molecular function is not fully understood. In the future, the chemo-physical properties of multipartite protein complexes involved in intracellular trafficking pathways need to be elucidated to provide insights into the physiological significance of them in the context of membrane trafficking.

Problem Statement and Hypothesis

Previously it was shown that deletion of *VPS1* leads to recycling defects of Snc1, an early endosome marker (Burston et al., 2009; Rooij et al., 2010; Saimani et al., 2017). Similarly, cells lacking Vps1 demonstrated mistargeting of Vps10, a late endosome marker (Parlati et al., 2002; Chi et al., 2014). Although Vps1 has been proposed to function as a membrane scission factor for decades, much attention has been given lately to a new crucial role of Vps1 acting in the homotypic fusion of vacuolar membranes (Peters et al., 2004; Kulkarni et al., 2014) . These observations raise the question of whether Vps1 is required for membrane fusion of other organelles including the endosome-derived vesicle fusion to the TGN. Endosome to Golgi trafficking is shown to be regulated by Ypt6, mammalian Rab6 homologue (Luo and Gallwitz, 2003). Therefore, it is not surprising to find that cells lacking Ypt6 fail to complete the retrograde traffic of Snc1 (Gossing et al., 2013). In light of the previous finding from our lab that double deletion of *VPS1* and *YPT6* leads to synthetic lethality (not published), one can hypothesize that Ypt6 (the main regulatory of cargo trafficking of the endosome-to-TGN) functions together with Vps1 to facilitate the endosome-derived vesicle tethering and fusion to the Golgi.

Using a diverse array of cell and molecular methods, my results from study will provide possible answers for the following major scientific questions;

1) Does Vps1 physically interact with Ypt6?
2) Are there any particular domains of Vps1 or regions of Ypt6 implicated in the possible physical interaction?
3) Is the possible interaction between Vps1 and Ypt6 affected by Ypt6 localizing at the Golgi?

4) Will Vps1 function upstream or downstream of Ypt6?

5) What is the physiological significance of the Vps1 and Ypt6 interaction?

6) If Vps1 is implicated during the endosome-derived vesicle fusion at the Golgi, does it also interact with the fusion proteins called SNAREs?

In my results and discussion sections, I present evidence of a physical interaction between Vps1 and Ypt6. Furthermore, I found that Vps1 and Ypt6 function redundantly for the endosome-to-TGN trafficking of Snc1 through their GTPase activity. In addition to Ypt6, Vps1 interacts with Vti1 and Snc2 SNAREs, indicating a role for Vps1 in the later stages of the endosome-derived vesicle tethering/fusion at the TGN.

MATERIALS AND METHODS

Construction of Plasmids and Yeast Strains

The corresponding DNA sequences of Vps1 or its fragments were fused to the GAL4 DNA-binding domain (BD) of the bait plasmid pGKBT7 (KKD 0099), between the *EcoR*I and *BamH*I restriction sites. DNA sequences that code for full-length Ypt6, Ypt6 (1-72 amino acid), Ypt6 (73-142 amino acid), Ypt6 (143-215 amino acid), Vti1 (1-130 amino acid), Vti1 (1-186 amino acid), Vti1 (130-186 amino acid), Tlg1 (1-131 amino acid), Tlg2 (1-35 amino acid), Snc2 (1-52 amino acid), Snc2 (1-96 amino acid), Snc2 (28-52 amino acid), and Snc2 (52-96 amino acid) were inserted into the downstream of the GAL4 DNA-activation domain (AD) (Stein et al., 2009) of the prey vector pGADT7 (KKD 0083) by using the *EcoR*I and *BamH*I restriction enzyme sites. For confirmation of the presence of the gene of interest into the bait or prey vector, a standard restriction enzyme digestion protocol was used. All positive prey and bait vectors were introduced into Y187 yeast strain (KKY 1255) and Y2H Gold Yeast strain (KKY 1254), respectively, by using the one-step transformation protocol. The resulting transformants that carry the prey or the bait vector was plated onto either media lacking leucine (SD/-Leu) or media lacking tryptophan (SD/-Trp), respectively, for 3-5 days at 30˚C. The positive colony screen was done by a colony PCR. All yeast strains constructed by these methods are listed in Table 1.

For creating p416-TEF-mRFP-Ypt6 (KKD 0315) vector, pOK489 (mRFP-Cps1) (KKD 0143) plasmid was digested with *EcoR*I and *Xho*I enzymes to remove *CPS1* sequence, and the amplified PCR product of YPT6 was ligated into the linearized

plasmid. To construct gene deletion strains, such as *vps1*Δ (KKY 0352) and *ypt6*Δ (KKY 0811), a standard PCR-based gene tagging method was performed. The target gene was replaced with a KanMX6 module. To tag 3'end of the *VPS10* with GFP, the same standard PCR-based gene tagging method was used. Amplification of the GFP sequence was performed using pFA6a-GFP (S65T)-TRP1 (KKD 0007) plasmid as a template.

Three 2-micron plasmids, pCAV30-Vps1 (KKD 0090), pCAV33-*vps1*-Δ*C* (KKD 0092), and pCAV29-*vps1*-Δ*N* (KKD 0089), were used for the overexpression of full-length Vps1, C-terminal half truncated Vps1 by deleting at 356th codon of Vps1, and N-terminal half truncated Vps1 by deleting codons of 19th-356th, respectively. P_{TPI1}-GFP-SNC1 URA3 CEN (KKD 0064) and P_{TPI1}-GFP-SNC1pm URA3 CEN (KKD 0062) plasmids were donated by Dr. Tanaka from Hokkaido University. Lastly, pFA6a-GFP (S65T)-TRP1 (KKD 0007) plasmid was received as a gift from Dr. Longtine (University of North Carolina). All plasmid strains mentioned above are listed on Table 2.

Yeast Two-Hybrid Screening

Positive transformants that carry prey vectors (AD-fused preys) were mated with yeast strains harboring bait vectors on a culture plate that lacks both leucine and tryptophan (SD/-Leu-Trp) (DDO) for 3-5 days at 30°C. Two to three positive colonies that grew on DDO plates were cultured in DDO broth at 30°C for 1-2 days until they reached an optical density at 600nn (OD_{600}) of 1.5. Serial dilutions of the cell cultures by a factor of 3 were performed in a 96 well plate. Those diluted cells were spotted onto DDO, TDO (SD/-Leu-Trp-His), and QDO (SD/-Leu-Trp-His-Ade) plates. After 3-5 days of incubation at 30°C, the extent of cell growth on those plates was determined using a

Kodak Image Station 4000MM or an Azure c300 Chemiluminescent Western Blot Imaging System.

Site-Directed Point Mutagenesis

Phusion Site-Directed Mutagenesis Kit (Thermo Scientific) was used to introduce base substitution mutations in a desired gene. Briefly, pGADT7-Ypt6 (KKD 0082) plasmid, a PCR template, was annealed with a pair of primers, one of which carries a base substitution. Subsequent extension via Phusion Hot Start DNA Polymerase was completed to produce the following three pGADT7 vectors carrying a base substitution in *YPT6* gene: pGADT7-Ypt6^{T24N} (KKD 0251), pGADT7-Ypt6^{Q69L} (KKD 0252), and pGADT7-Ypt6^{G139E} (KKD 0174). Agarose gel electrophoresis was used to verify the success of the PCR amplification. The amplified PCR product was ligated by T4 DNA Ligase, and a standard bacterial transformation protocol was used to introduce the ligated PCR product into Stellar Competent *E. coli* (Clontech) cells. These cells were inoculated onto Luria Broth (LB)-ampicillin agar plates and incubated at 37°C overnight. Two to three transformants were then transferred into 3 ml LB-ampicillin media and were grown overnight at 37°C. The mutated plasmid DNA was extracted from these colonies by the QIAprep® Spin Miniprep Kit protocol (Qiagen). The isolated plasmid DNA products were sent to a DNA sequencing facility (Eurofins Genomics) to confirm that the desired mutations had occurred. Similarly, base substitution mutant strains carrying pCAV-Vps1^{K42E} (KKD 0276), pCAV-Vps1^{S43N} (KKD 0275), or pCAV-Vps1^{G315D} (KKD 0274) were generated using pCAV30 (KKD 0090) plasmid as a template. The mutated plasmids

of *YPT6* and *VPS1* were then introduced into appropriate yeast strains via the one-step transformation protocol mentioned previously.

Fluorescence Microscopy and Data Quantification

Fluorescently labeled cells were visualized using a spinning confocal microscope equipped with a Yokogawa CSUX1 spinning disk head, a 100X oil immersion PlanApo objective lens, and an ImagEM camera. The exposure time for single-channel imaging was set to 50ms for all images. In the case of simultaneous two-color imaging, green and red emission signals were separated by a two-channel emission splitting system (DV2, Photometrics). The exposure time for a red emission signal was set to 200ms, whereas the exposure time for the green signal was set to 80ms.

Quantification of the extent of GFP-Snc1 polarization was done by monitoring GFP-Snc1 distribution patterns using fluorescence microscopy. In normal or polarized cells, GFP-Snc1 is polarized at the bud membrane, while non-polarized or depolarized cells display no GFP-Snc1 polarization at the bud.

To investigate the effect of loss of Vps1 and Ypt6 on the late endosome-derived vesicle trafficking to the TGN, Vps10 was used as a late endosome-to-Golgi recycling marker. Yeast budding cells that express Vps10-GFP were quantified by marking down whether the cell shows a ring-like structure. Vps10-GFP forming a ring-like structure in the cells was used as an indicator of Vps10 mistargeting to the vacuole. In these cells, Vps10-GFP puncta numbers were also noted, and the average of these puncta in each cell strain was calculated.

All data generated using fluorescence microscopy were repeated in three individual sets. For each strain, 30-50 budding yeast cells were quantified per each set. Then, the mean and standard deviation of the three-data sets were determined using Excel. Student's *T*-test (2 tails, two sample unequal variance) was performed using Excel and results were reported as *p*-values. The *P*-value ≤ 0.01 is represented with three asterisks (***).

RESULTS

The Physical Interaction between Vps1 and Ypt6

Cells lacking Vps1 showed disrupted trafficking of the *v*-SNARE Snc1 from the endosome to the Golgi (Furuta et al., 2007). Similarly, in *ypt6*Δ cells, Snc1 traffic toward the Golgi was affected negatively (Suda et al., 2013). Codeletion of *VPS1* and *YPT6* genes led to synthetic lethality (personal communication with Kim lab), suggesting a functional link between Vps1 and Ypt6 via a physical interaction. To test whether Vps1 and Ypt6 physically interact with each other, cells coexpressing BD-Vps1 and AD-Ypt6 were applied onto selective plates of DDO and TDO. These diploid cells grew on TDO plates, as positive control cells coexpressing BD-p53 and AD-T (Wiederhold and Fasshauer, 2009), indicating that Vps1 and Ypt6 do physically interact *in vivo* (Figure 3A). A negative control strain coexpressing both BD-Lam and AD-T, which have been shown not to interact (Alpadi et al., 2013; Krämer and Ungermann, 2011), did not grow on TDO plates. Two other negative control strains expressing either AD-Ypt6 or BD-Vps1 did not show growth on the DDO or TDO plates either (Figure 3A).

Vps1 consists of three domains, a GTPase catalytic domain (1-340 amino acid), a middle domain (341-614 amino acid), and a GTPase effector domain (615-704 amino acid) (Banh et al., 2017). To map the Vps1 region that binds to Ypt6, cells carrying AD-Ypt6 and a BD-fused domain of Vps1 were constructed. All three domains of Vps1 showed physical interaction with full-length Ypt6 *in vivo* (Figure 3A). To identify the minimal region of Ypt6 that interacts with Vps1, we constructed cells coexpressing an AD-fused Ypt6 fragment (AD-Ypt6 (1-72 amino acid), AD-Ypt6 (73-142 amino acid), or

AD-Ypt6 (143-215 amino acid)) and BD-Vps1. All three fragments of Ypt6 displayed interaction with Vps1 (Figure 3B). However, none of the Vps1 domains interacted with Ypt6 segments (Figure 3C-E), suggesting that full-length Vps1 or Ypt6 is required for its binding with any fragment of the other binding partner.

Fusion of endosome-derived vesicles with the TGN requires the energy driven by Ypt6-mediated GTP hydrolysis (Hutagalung and Novick, 2011). A GTP-bound active Ypt6 localizes and functions at the TGN, whereas an inactive GDP-bound Ypt6 is found in the cytoplasm (Bui et al., 2012). Our working hypothesis was that only the active version of Ypt6 would show interaction with Vps1. Two other groups of researchers purposed that a substitution of the 69th amino acid), glutamine (Q), of Ypt6 with leucine (L), leads to the formation of a constitutively active version of Ypt6 (*ypt6*^{Q69L}) (Protopopov et al., 1993; Yang and Rosenwald, 2016). In contrast, T24N or G139E mutations caused the production of an inactive version of Ypt6 (*ypt6*^{T24N} or *ypt6*^{G139E}) (Kawamura et al., 2014; Luo and Gallwitz, 2003; Yang and Rosenwald, 2016). Cells coexpressing an AD-fused *ypt6* mutant *(ypt6*^{Q69L}, *ypt6*^{T24N}, or *ypt6*^{G139E}) with BD-Vps1 grew on both DDO and TDO plates (Figure 3F), indicating that both GTP- and GDP-bound forms of Ypt6 bind to Vps1. This suggests that the interaction of Ypt6 and Vps1 does not depend on the status of Ypt6 activity (Figure 3F).

The Functional Relationship between Vps1 and Ypt6

Snc1 is a vesicle SNARE (*v*-SNARE) that mainly localizes at the plasma membrane of the bud, thus displaying a polarized distribution (Figure 4A). Post-internalized Snc1 is delivered from the early endosome to the TGN prior to recycling

back to the plasma membrane. Snc1 recycling defects, manifested by its mislocalization, were previously observed in both *ypt6*Δ and *vps1*Δ cells, indicating that both Ypt6 and Vps1 act on Snc1 recycling. Consistent with this notion, mislocalization or depolarization of GFP-Snc1, a phenotypic defect of GFP-Snc1 upon loss of Vps1 or Ypt6, was observed in our experiments. 68-70% of WT cells showed a polarized pattern of GFP-Snc1 (Figures 4 and 5), while levels of GFP-Snc1 polarization in *ypt6*Δ (25.94±9.08%) and *vps1*Δ cells (20.63±1.92%) were drastically reduced (Figure 4 and 5).

Given the absence of Ypt6 or Vps1 resulted in essentially the same phenotype of GFP-Snc1 polarization defect, we reasoned that Vps1 might act as a Ypt6 effector in a sequential pathway of GFP-Snc1 traffic, or *vice versa*. In a sequential pathway, overexpression of a downstream effector could overcome any phenotypic defects caused by loss or malfunction of its upstream factor. Firstly, it was observed that overexpression of full-length Vps1 (51.06±6.32%) or the N-terminal half of Vps1 (52.05±6.5%) in the *ypt6*Δ background significantly rescued GFP-Snc1 polarization defects caused by the loss of Ypt6 (Figure 4A and B). However, overexpression of the C-terminal half of Vps1 (27.5±9.01%) resulted in no significant rescue (Figure 4A and B). Interestingly, overexpression of Ypt6 in the *vps1*Δ background also led to a substantial rescue of GFP-Snc1 polarization defects (62.22±3.84%) (Figure 5A and B), and as expected, the reintroduction of Vps1 (66.98±10.76%) in *vps1*Δ led to a significant recovery of GFP-Snc1 polarization levels (Figure 5A and B). Together, it appears that Vps1 and Ypt6 do not function in a sequential pathway.

Snc1 recycling involves its endocytic targeting to the early endosome, followed by a retrograde traffic toward the Golgi and then a traffic toward the plasma membrane.

We tested the possibility that GFP-Snc1 trafficking to the plasma membrane, a part of its recycling, is compromised in *vps1*Δ and *ypt6*Δ cells. For this study, we introduced into WT, *vps1*Δ, and *ypt6*Δ cells GFP-Snc1pm, which is a Snc1 endocytic mutant that is targeted to the plasma membrane properly but is not endocytosed. In all these strains GFP-Snc1pm was found at the plasma membrane of cells, reflecting no defects in the GFP-Snc1 secretory pathway, from the Golgi to the plasma membrane (Figure 6). Considering that wild type GFP-Snc1 was found in cytosolic puncta in *vps1*Δ and *ypt6*Δ cells, we also excluded the possibility of endocytic defects of Snc1 in those mutant cells (Figure 4A and 5A). Altogether, the data suggest that loss of Vps1 or Ypt6 leads to a retrograde GFP-Snc1 trafficking defect toward the Golgi.

Vps1 GTPase Activity is Essential for Snc1 Retrograde Recycling

Due to the significant recovery of the polarized phenotype of GFP-Snc1 by overexpressing the N-terminal half of Vps1 alone, but not by the C-terminal half of Vps1 in *ypt6*Δ cells (Figure 4), we hypothesized that the GTPase activity of Vps1 is necessary for the GFP-Snc1 retrograde recycling. Since three residues, K42, S43, and G315, in the N-terminal half of Vps1 are implicated in GTP hydrolysis, we assessed the effect of the mutation of these residues on GFP-Snc1 recycling. Using a site-directed mutagenesis system, we cloned Vps1 GTPase mutants, including $vps1^{K42N}$, $vps1^{S43N}$, and $vps1^{G315D}$. These Vps1 mutants were introduced into *vps1*Δ cells expressing GFP-Snc1 (Figure 7).

These *vps1* mutant strains expressing $vps1^{K42N}$, $vps1^{S43N}$, or $vps1^{G315D}$ displayed 21.09±6.26%, 19.04±4.61%, or 17.75±5.23% of GFP-Snc1 polarization, respectively, compared with *vps1*Δ cells (27.61±7.95%) (Figure 7A and B). Consistent with the

previous data (Figure 7B), when full-length Vps1 was overexpressed in the *vps1*Δ background cells, a significant recovery of GFP-Snc1 polarization (64.84±6.84%) was observed, similar to WT cells (71.98±9.83%) (Figure 7A and B). These results indicate that Vps1 GTPase mutant variants did not rescue the GFP-Snc1 polarization defects caused by loss of Vps1, pointing to the necessity of GTPase activity of Vps1 for Snc1 recycling.

Next, we investigated whether the Vps1 GTPase activity is required to rescue GFP-Snc1 polarization defects caused by loss of Ypt6 (Figure 8). Overexpression of $vps1^{K42N}$, $vps1^{S43N}$, or $vps1^{G315D}$ in the *ypt6*Δ background cells displayed 37.05±6.96%, 31.12±5.50%, or 18.07±7.96% of GFP-Snc1 polarization, respectively (Figure 8A and B). On the contrary, a significant rescue of the aberrant phenotype of GFP-Snc1 was seen in *ypt6*Δ cells overexpressing full-length Vps1 (47.26±5.77%), compared with *ypt6*Δ (28.11±11.62%) (Figure 8A and B). Taken together, it can be suggested that both Vps1 and Ypt6 act for Snc1 recycling as a GTPase.

Vps1 is Required for Proper Vps10 Recycling

To assess whether Vps1 plays a role in the traffic from the late endosome to the Golgi, we constructed WT and *vps1*Δ cells to express Vps10-GFP and examined its localization. It was previously shown that in *vps1*Δ cells Vps10-GFP is mostly mistargeted to the rim of the vacuole, forming one or more ring-like structures that indicates an endosome-to-Golgi traffic defect (Arlt et al., 2015; Chi et al., 2014). Consistently, 57.77±5.09% of *vps1*Δ cells displayed vacuolar rings stained with Vps10-GFP, compared to WT cells (2.42±1.57%) (Figure 9A and B). The percentage of cells

with Vps10-GFP ring-like structure(s) in *vps1*Δ background cells expressing *vps1* mutant proteins (*vps1*^{K42N}, *vps1*^{S43N}, or *vps1*^{G315D}) were 64.44±6.93%, 62.22±1.925, or 68.88±15.03%, respectively (Figure 9A and B). These results indicate that Vps1 GTPase mutants lead to a failure to rescue the Vps10-GFP mislocalization defects caused by loss of Vps1. Therefore, Vps1 GTPase function is crucial for the retrograde trafficking of Vps10 from the late endosome to the Golgi.

Vps1 Physically Interacts with Vti1 and Snc2 SNAREs

To further investigate whether Vps1 is implicated in endosome-derived vesicle fusion with the TGN, the last step of endosome-to-Golgi traffic, we examined the possibility that Vps1 interacts with 4 SNAREs that form a *trans*-SNARE complex at the TGN. These SNAREs include a *v*-SNARE Snc2, and three target SNAREs Vti1, Tlg1, and Tlg2. The N-termini of Tlg1, Tlg2, Vti1, and Snc2 are cytosolic, while the C-terminal domains of these SNAREs are embedded in the membrane. The cytosolic domain of a SNARE protein is mostly responsible for regulating essential functions of the SNARE complex. To test whether Vps1 interacts with these cytosolic domains of the SNAREs, we constructed cells coexpressing BD-Vps1 and AD-fused N-terminal domain of each SNARE, Tlg1 (1-131 amino acid), Tlg2 (1-35 amino acid), Snc2 (1-96 amino acid), or Vti1 (1-186 amino acid). The resulting cells were applied onto DDO, TDO, and QDO plates (Figure 10A). As the case for the positive control strain, cells that coexpress BD-Vps1 and AD-Snc2 (1-96 amino acid) or AD-Vti1(1-186 amino acid) grew on selective plates of TDO and QDO (Figure 10A), indicating that Vps1 interacts with both the cytosolic domains of Snc2 (1-96 amino acid) and Vti1 (1-186 amino acid).

The cytosolic domain of Vti1 consists a three-helix bundle (1-130 amino acid) and a SNARE motif (130-186 amino acid). Each of these two sub-regions of Vti1 was cloned into the AD-vector. Cells harboring BD-Vps1 and an AD-fused domain of Vti1 (AD-Vti1 (1-130 amino acid) or AD-Vti1 (130-186 amino acid)) were applied onto DDO, TDO, and QDO plates, as well as the same positive and the negative control strain (Figure 10B). Additionally, to define the region of the cytosolic domain of Snc2 that is involved in binding to Vps1, we expressed Snc2 (1-28 amino acid), Snc2 (28-96 amino acid), and Snc2 (52-96 amino acid) truncations fused to AD prey vector and tested for Vps1 binding. Cells coexpressing cytosolic Snc2 domains (AD-Snc2 (1-28 amino acid), AD-Snc2 (28-96 amino acid), or AD-Snc2 (52-96 amino acid)) and BD-Vps1 were plated onto DDO, TDO, QDO plates (Figure 10B). Surprisingly, except the positive control strain, no growth was observed in TDO or QDO plates (Figure 10B), indicating that the full N-terminal region of Snc2 and Vti1 is required for their binding to Vps1.

DISCUSSION

The three-dimensional (3D) structure of a protein is crucial for its function, recruitment, and association with other proteins. Lines of evidence demonstrate that Vps1 locates at the TGN (Lukehart et al., 2013; Arlt et al., 2015; Goud Gadila et al., 2017), but its function there has been poorly understood. Therefore, finding its binding partners residing at the TGN can shed some light on how Vps1 may function at the TGN. In this study, it was found that full-length Vps1 binds to full-length Ypt6 and vice versa. Additionally, all truncated versions of Vps1 interact with full-length Ypt6. Likewise, three truncated Ypt6 proteins bind to full-length Vps1, suggesting that these two proteins contain multiple binding regions to each other. However, domain mapping experiments in this study using truncated Vps1 and Ypt6 to identify specific regions for their interactions were not successful. One possible explanation for this is that producing truncated versions of a protein may lead to misfolding. Therefore, the structure of a truncated version of Vps1 or Ypt6 may not resemble the 3D structure of its counterpart of the corresponding full-length protein, not presenting regions of interaction with its binding partner. Though expression of a truncated version of a protein might disrupt its structure and function, interpreting the impact of their expression in the cells could shed light on highlighting the functional aspect of the normal protein. As such, a group of scientists engineered cells to express a truncated version of the dynamin-like protein Dnm1 to assess any phenotypic defects caused by the removal of a novel motif called insert-B, which interacts with Mdv1 (mitochondrial adaptor-1) to facilitate vesicle fission at the mitochondrion in yeast (Derivery et al., 2012). The loss of the motif not only

resulted in attenuating Dnm1-Mdv1 interaction but also severely interrupting Dnm1's recruitment to the mitochondrion, leading to a conclusion that insert-B motif plays a role in Dnm1 recruitment.

Another possible explanation for the abolished interaction between a Vps1 domain and a truncated version of Ypt6 is that these truncated versions do not present full binding region for the other binding fragments, thereby disrupting their physical association.

Functional Relationship of Vps1 with Ypt6

It has been previously shown that cells lacking *VPS1* or *YPT6* do not properly recycle Snc1, a *v*-SNARE to be transported from the early endosome to the TGN (Liu et al., 2006; Rooij et al., 2010; Lukehart et al., 2013; Saimani et al., 2017). These observations in conjunction with the findings that both proteins locate at the TGN (Lukehart et al., 2013; Arlt et al., 2015; Goud Gadila et al., 2017) raise the question of whether Vps1 and Ypt6 function cooperatively with each other. My results show that Snc1 distribution defects caused by loss of Vps1 were rescued by overexpression of Ypt6, and *vice versa*. Based on these results, it was hypothesized that Vps1 or Ypt6 does not function as an upstream or a downstream factor for the other, rather they might function in parallel pathways or redundantly in a converging manner to their common downstream effector to positively impact endosome tethering and fusion at the TGN. A recent double deletion assay in which both *YPT6* and *VPS1* were deleted led to synthetic lethality (personal communication with Kim lab), which also supports the hypothesis mentioned above. In accordance with the hypothesis of functional redundancy on Snc1

trafficking, my study showed that overexpression of full-length Vps1, but not with a GTPase mutant of Vps1 (*vps1*^{K42N}, *vps1*^{S43N}, or *vps1*^{G315D}), was sufficient enough to rescue recycling defects of Snc1 in *vps1*Δ or *ypt6*Δ cells. This result indicates that both Ypt6 and Vps1 functions as a GTPase for Snc1 trafficking to the TGN and that the GTPase activity of Vps1 may function redundantly with that of Ypt6. The functional significance of Ypt6 GTPase activity in this traffic was previously demonstrated by expression of a continuously active mutant version of Ypt6 (*ypt6*^{Q69L}), which does not rescue the phenotypic defects of Snc1 in *ypt6*Δ cells (Tani and Kuge, 2012).

What are the possible common downstream effectors of Vps1 and Ypt6, functioning in endosome-derived vesicle tethering/fusion at the TGN? A recent study showed that Vps1 interacts with Vps51, a subunit of the TGN tether GARP and that deletion of Vps1 disturbed the targeting of Vps51 to the TGN (Saimani et al., 2017). Furthermore, under this condition Tlg1, a *t*-SNARE at the TGN, is partially mislocalized to the vacuole (Saimani et al., 2017). This set of data supports the notion that Vps1 might act upstream of the tether. Interestingly, it is well-known that Ypt6 serves as an upstream regulator of the GARP through its interaction with Vps52, another subunit of the tether (Perez-Victoria et al., 2008). Taken together, it is clear that both Vps1 and Ypt6 act redundantly on the GARP, though their specific binding partners are different. Importantly, the present study revealed that Vps1 physically associates with two SNAREs, Vti1 and Snc2, acting on the fusion event at the TGN, further strengthening the notion that Vps1 functions upstream of the tethering and fusion or facilitates the downstream steps.

Establishing a Niche for Vps1 at the TGN

Recent studies have revealed the Vps1's role in the homotypic fusion of vacuolar membrane. It has been found that Vps1 is necessary for mediating the interaction between two vacuolar SNAREs, Vam3 and Nvy1 (Alpadi et al., 2013). In the presence of a self-assembly defective mutant (I649K) or a GTPase-mutant (*vps1*^{K42A}) of Vps1, the interaction between Vam3 and Nvy1 was significantly compromised, indicating that both oligomerization and GTPase activity of Vps1 are crucial for proper binding between these two SNAREs. A follow-up study showed that deletion or self-assembly mutants (*vps1*^{I649K}, *vps1*^{K642L}, and *vps1*^{Y628F}) of Vps1 led to a significant reduction of the interaction of Vam3 with the HOPS (homotypic fusion and protein sorting) complex, a tether at the vacuole (Kulkarni et al., 2014). These lines of investigation signify that the oligomerization of Vps1 has an impact on both SNARE-SNARE and SNARE-tether interactions, which regulates the homotypic fusion of vacuolar membranes (Alpadi et al., 2013; Kulkarni et al., 2014). It is important to note that these findings are consistent with a new paradigm that states that proper membrane fusion requires a multipartite complex including tethers, GTPases, SNAREs, and other accessory proteins for transport vesicle fusion at the target membrane (Chia and Gleeson, 2014). Membrane tethering and fusion at any location in the cells would require similar multipartite complex as seen at the vacuole. This notion allows me to postulate the possibility that a functional multipartite complex, which contains an array of proteins regulating tethering/fusion, exists at the TGN. I propose that the multipartite protein complex at the TGN is composed of Ypt6, Vps1, the GARP, and SNAREs (Figure 11A). In this complex Ypt6, a well-known main regulator of the endosome-to-TGN trafficking, interacts with its downstream effector

Vps52 (Perez-Victoria et al., 2008), and in turn Vps52 is associated with Vps51 that binds to Tlg1, thereby creating a local protein network linking the upstream regulator to the tethering/fusion machinery at the TGN (Figure 11B) (Siniossoglou and Pelham, 2001). As the case for the vacuolar homotypic fusion, Vps1 appears to serve as a multi-adhesive factor playing a role in securing the connection between these components because it interacts with Ypt6, Vps51, Snc2, and Vti1 (Figure 11B). Considering that the connection of Ypt6 to Vps52 and the linkage of Vps1 with Vps51, I envision that Ypt6 and Vps1 act on Vps52 and Vps51, respectively, to ensure a tight assembly of the multipartite complex (Figure 11A and B). Therefore, the effects of these connections to the GARP are in favor of assisting the last step of the endosome-to-TGN traffic, namely fusion that is mediated by the SNAREs at the TGN (Figure 11C). Taken together, all these data support the idea that Vps1 plays a fundamental role for the membrane tethering/fusion at the TGN.

REFERENCES

Abascal-Palacios, G, Schindler, C, Rojas, AL, Bonifacino, JS, and Hierro, A (2013) Structural Basis for the Interaction of the Golgi-Associated Retrograde Protein (GARP) Complex with the t-SNARE Syntaxin 6. Structure (London, England : 1993) 21, 1698-1706.

Albuquerque, CP, Smolka, MB, Payne, SH., Bafna, V, Eng, J, and Zhou, H (2008) A multidimensional chromatography technology for in-depth phosphoproteome analysis. Molecular and cellular proteomics : MCP 7, 1389-1396.

Alpadi, K, Kulkarni, A, Comte, V, Reinhardt, M, Schmidt, A, Namjoshi, S, Mayer, A, and Peters, C (2012) Sequential analysis of trans-SNARE formation in intracellular membrane fusion. PLoS biology 10, e1001243.

Alpadi, K, Kulkarni, A, Namjoshi, S, Srinivasan, S, Sippel, KH, Ayscough, K, Zieger, M, Schmidt, A, Mayer, A, Evangelista, M, et al. (2013) Dynamin-SNARE interactions control trans-SNARE formation in intracellular membrane fusion. Nature communications 4, 1704-1704.

Antonny, B, Burd, C, De Camilli, P, Chen, E, Daumke, O, Faelber, K, Ford, M, Frolov, VA, Frost, A, Hinshaw, J.E, et al. (2016) Membrane fission by dynamin: what we know and what we need to know. Embo j 35, 2270-2284.

Arlt, H, Reggiori, F, and Ungermann, C (2015) Retromer and the dynamin Vps1 cooperate in the retrieval of transmembrane proteins from vacuoles. J Cell Sci 128, 645-655.

Baker, RW, and Hughson, FM.(2016) Chaperoning SNARE assembly and disassembly. Nature reviews Molecular cell biology 17, 465-479.

Baker, RW, Jeffrey, PD, and Hughson, FM (2013) Crystal Structures of the Sec1/Munc18 (SM) Protein Vps33, Alone and Bound to the Homotypic Fusion and Vacuolar Protein Sorting (HOPS) Subunit Vps16*. PloS one 8, e67409.

Banh, BT, McDermott, H, Woodman, S, Gadila, SKG, Saimani, U, Short, JCW, and Kim, K (2017) Yeast dynamin interaction with ESCRT proteins at the endosome. Cell Biology International 41, 484-494.

Barr, F, and Lambright, DG (2010) Rab GEFs and GAPs. Current opinion in cell biology 22, 461-470.

Barr, VA, Phillips, SA, Taylor, SI, and Haft, CR (2000) Overexpression of a novel sorting nexin, SNX15, affects endosome morphology and protein trafficking. Traffic 1, 904-916.

Barrowman, J, Bhandari, D, Reinisch, K, and Ferro-Novick, S (2010) TRAPP complexes in membrane traffic: convergence through a common Rab. Nat Rev Mol Cell Biol 11, 759-763.

Bashkirov, PV, Akimov, SA, Evseev, AI, Schmid, SL, Zimmerberg, J, and Frolov, VA (2008) GTPase cycle of dynamin is coupled to membrane squeeze and release, leading to spontaneous fission. Cell 135, 1276-1286.

Benjamin, JJR, Poon, PP, Drysdale, JD, Wang, X, Singer, RA, and Johnston, GC (2011) Dysregulated Arl1, a regulator of post-Golgi vesicle tethering, can inhibit endosomal transport and cell proliferation in yeast. Molecular Biology of the Cell 22, 2337-2347.

Bonifacino, JS, and Hierro, A (2011) Transport According to GARP: Receiving Retrograde Cargo at the Trans-Golgi Network. Trends in cell biology 21, 159-167.

Bonifacino, JS, and Rojas, R (2006) Retrograde transport from endosomes to the trans-Golgi network. Nat Rev Mol Cell Biol 7, 568-579.

Brown, FC, Schindelhaim, CH, and Pfeffer, SR (2011) GCC185 plays independent roles in Golgi structure maintenance and AP-1–mediated vesicle tethering. The Journal of Cell Biology 194, 779-787.

Brunet, S, and Sacher, M (2014) Are all multisubunit tethering complexes bona fide tethers? Traffic 15, 1282-1287.

Buggia-Prévot, V, and Thinakaran, G (2015) Significance of transcytosis in Alzheimer's disease: BACE1 takes the scenic route to axons. BioEssays : news and reviews in molecular, cellular and developmental biology 37, 888-898.

Bui, HT, Karren, MA, Bhar, D, and Shaw, JM (2012) A novel motif in the yeast mitochondrial dynamin Dnm1 is essential for adaptor binding and membrane recruitment. The Journal of Cell Biology 199, 613-622.

Burd, C, and Cullen, PJ (2014) Retromer: a master conductor of endosome sorting. Cold Spring Harbor perspectives in biology 6.

Burd, CG (2011) Physiology and pathology of endosome-to-Golgi retrograde sorting. Traffic 12, 948-955.

Burston, HE, Maldonado-Baez, L, Davey, M, Montpetit, B, Schluter, C, Wendland, B, and Conibear, E. (2009) Regulators of yeast endocytosis identified by systematic quantitative analysis. J Cell Biol 185, 1097-1110.

Camley, BA, and Brown, FL (2011) Beyond the creeping viscous flow limit for lipid bilayer membranes: theory of single-particle microrheology, domain flicker spectroscopy, and

long-time tails. Physical review E, Statistical, nonlinear, and soft matter physics 84, 021904.

Chappie, JS, and Dyda, F (2013) Building a fission machine – structural insights into dynamin assembly and activation. Journal of Cell Science 126, 2773-2784.

Chappie, JS, Mears, JA, Fang, S, Leonard, M, Schmid, SL, Milligan, RA, Hinshaw, JE, and Dyda, F (2011) A pseudo-atomic model of the dynamin polymer identifies a hydrolysis-dependent powerstroke. Cell 147, 209-222.

Chen, DC, Yang, BC, and Kuo, TT (1992) One-step transformation of yeast in stationary phase. Curr Genet 21, 83-84.

Cheung, P-yP, Limouse, C, Mabuchi, H, and Pfeffer, SR (2015) Protein flexibility is required for vesicle tethering at the Golgi. eLife 4, e12790.

Cheung, P-yP, and Pfeffer, SR (2016) Transport Vesicle Tethering at the Trans Golgi Network: Coiled Coil Proteins in Action. Frontiers in Cell and Developmental Biology 4, 18.

Cheung, PY, Limouse, C, Mabuchi, H, and Pfeffer, SR (2015) Protein flexibility is required for vesicle tethering at the Golgi. eLife 4.

Chi, RJ, Liu, J, West, M, Wang, J, Odorizzi, G, and Burd, CG (2014) Fission of SNX-BAR-coated endosomal retrograde transport carriers is promoted by the dynamin-related protein Vps1. J Cell Biol 204, 793-806.

Chia, PZC, Gasnereau, I, Lieu, ZZ, and Gleeson, PA (2011) Rab9-dependent retrograde transport and endosomal sorting of the endopeptidase furin. Journal of Cell Science 124, 2401-2413.

Chia, PZC, and Gleeson, PA (2014) Membrane tethering. F1000Prime Reports 6, 74.

Chowdhury, S, Ketcham, SA, Schroer, TA, and Lander, GC (2015) Structural organization of the dynein-dynactin complex bound to microtubules. Nature structural and molecular biology 22, 345-347.

Climer, LK, Dobretsov, M, and Lupashin, V (2015) Defects in the COG complex and COG-related trafficking regulators affect neuronal Golgi function. Frontiers in Neuroscience 9, 405.

Cocucci, E, Gaudin, R, and Kirchhausen, T (2014) Dynamin recruitment and membrane scission at the neck of a clathrin-coated pit. Mol Biol Cell 25, 3595-3609.

Cosen-Binker, LI, and Kapus, A (2006) Cortactin: The Gray Eminence of the Cytoskeleton. Physiology 21, 352-361.

Coutinho, MF, Prata, MJ, and Alves, S (2012) Mannose-6-phosphate pathway: a review on its role in lysosomal function and dysfunction. Molecular genetics and metabolism 105, 542-550.

Crevenna, AH, Blank, B, Maiser, A, Emin, D, Prescher, J, Beck, G, Kienzle, C, Bartnik, K, Habermann, B, Pakdel, M, et al. (2016) Secretory cargo sorting by Ca(2+)-dependent Cab45 oligomerization at the trans-Golgi network. The Journal of Cell Biology 213, 305-314.

Cullen, PJ, and Korswagen, HC (2012) Sorting nexins provide diversity for retromer-dependent trafficking events. Nat Cell Biol 14, 29-37.

Damke, H, Baba, T, Warnock, DE, and Schmid, SL (1994) Induction of mutant dynamin specifically blocks endocytic coated vesicle formation. J Cell Biol 127, 915-934.

Das, S, Yu, S, Sakamori, R, Stypulkowski, E, and Gao, N (2012) Wntless in Wnt secretion: molecular, cellular and genetic aspects. Frontiers in biology 7, 587-593.

de Boer, P, Hoogenboom, JP, and Giepmans, BNG (2015) Correlated light and electron microscopy: ultrastructure lights up! Nat Meth 12, 503-513.

Derivery, E, Helfer, E, Henriot, V, and Gautreau, A (2012) Actin polymerization controls the organization of WASH domains at the surface of endosomes. PloS one 7, e39774.

Derivery, E, Sousa, C, Gautier, JJ, Lombard, B, Loew, D, and Gautreau, A (2009) The Arp2/3 activator WASH controls the fission of endosomes through a large multiprotein complex. Developmental cell 17, 712-723.

Diaz, E, and Pfeffer, SR (1998) TIP47: a cargo selection device for mannose 6-phosphate receptor trafficking. Cell 93, 433-443.

Diaz-Salinas, MA, Silva-Ayala, D, Lopez, S, and Arias, CF (2014) Rotaviruses reach late endosomes and require the cation-dependent mannose-6-phosphate receptor and the activity of cathepsin proteases to enter the cell. J Virol 88, 4389-4402.

Efimov, A, Kharitonov, A, Efimova, N, Loncarek, J, Miller, PM, Andreyeva, N, Gleeson, P, Galjart, N, Maia, AR, McLeod, IX, et al. (2007) Asymmetric CLASP-dependent nucleation of noncentrosomal microtubules at the trans-Golgi network. Developmental cell 12, 917-930.

Eiseler, T, Hausser, A, De Kimpe, L, Van Lint, J, and Pfizenmaier, K (2010) Protein kinase D controls actin polymerization and cell motility through phosphorylation of cortactin. J Biol Chem 285, 18672-18683.

Elfrink, HL, Zwart, R, Cavanillas, ML, Schindler, AJ, Baas, F, and Scheper, W (2012) Rab6 is a modulator of the unfolded protein response: implications for Alzheimer's disease. J Alzheimers Dis 28, 917-929.

Faelber, K, Posor, Y, Gao, S, Held, M, Roske, Y, Schulze, D, Haucke, V, Noe, F, and Daumke, O (2011) Crystal structure of nucleotide-free dynamin. Nature 477, 556-560.

Fasshauer, D (2003) Structural insights into the SNARE mechanism. Biochimica et Biophysica Acta (BBA) - Molecular Cell Research 1641, 87-97.

Feyder, S, De Craene, J-O, Bär, S, Bertazzi, DL, and Friant, S (2015) Membrane Trafficking in the Yeast Saccharomyces cerevisiae Model. International Journal of Molecular Sciences 16, 1509-1525.

Follett, J, Norwood, SJ, Hamilton, NA, Mohan, M, Kovtun, O, Tay, S, Zhe, Y, Wood, SA, Mellick, GD, Silburn, PA, et al. (2014) The Vps35 D620N mutation linked to Parkinson's disease disrupts the cargo sorting function of retromer. Traffic 15, 230-244.

Fridmann-Sirkis, Y, Kent, HM, Lewis, MJ, Evans, PR, and Pelham, HR (2006) Structural analysis of the interaction between the SNARE Tlg1 and Vps51. Traffic 7, 182-190.

Fritzsche, M, Erlenkämper, C, Moeendarbary, E, Charras, G, and Kruse, K (2016) Actin kinetics shapes cortical network structure and mechanics. Science Advances 2.

Fukasawa, M, Cornea, A, and Varlamov, O (2013) Selective control of SNARE recycling by Golgi retention. FEBS Letters 587, 2377-2384.

Furuta, N, Fujimura-Kamada, K, Saito, K, Yamamoto, T, and Tanaka, K (2007) Endocytic recycling in yeast is regulated by putative phospholipid translocases and the Ypt31p/32p-Rcy1p pathway. Mol Biol Cell 18, 295-312.

Galjart, N (2005) CLIPs and CLASPs and cellular dynamics. Nat Rev Mol Cell Biol 6, 487-498.

Garcia-Castillo, MD, Tran, T, Bobard, A, Renard, HF, Rathjen, SJ, Dransart, E, Stechmann, B, Lamaze, C, Lord, M, Cintrat, JC, et al. (2015) Retrograde transport is not required for cytosolic translocation of the B-subunit of Shiga toxin. J Cell Sci 128, 2373-2387.

Gillingham, AK, and Munro, S (2016) Finding the Golgi: Golgin Coiled-Coil Proteins Show the Way. Trends in cell biology 26, 399-408.

Girard, E, Chmiest, D, Fournier, N, Johannes, L, Paul, J-L, Vedie, B, and Lamaze, C (2014) Rab7 Is Functionally Required for Selective Cargo Sorting at the Early Endosome. Traffic 15, 309-326.

Gossing, M, Chidambaram, S, and Fischer von Mollard, G (2013) Importance of the N-terminal domain of the Qb-SNARE Vti1p for different membrane transport steps in the yeast endosomal system. PloS one 8, e66304.

Goud Gadila, SK, Williams, M, Saimani, U, Delgado Cruz, M, Makaraci, P, Woodman, S, Short, JC, McDermott, H, and Kim, K (2017) Yeast dynamin Vps1 associates with clathrin to facilitate vesicular trafficking and controls Golgi homeostasis. European journal of cell biology 96, 182-197.

Grimaldi, AD, Maki, T, Fitton, BP, Roth, D, Yampolsky, D, Davidson, MW, Svitkina, T, Straube, A, Hayashi, I, and Kaverina, I (2014) CLASPs are required for proper microtubule localization of End-binding proteins. Developmental cell 30, 343-352.

Guerra, F, and Bucci, C (2016) Multiple Roles of the Small GTPase Rab7. Cells 5, 34.

Halemani, ND, Bethani, I, Rizzoli, SO, and Lang, T (2010) Structure and dynamics of a two-helix SNARE complex in live cells. Traffic 11, 394-404.

Hanne, J, Falk, HJ, Görlitz, F, Hoyer, P, Engelhardt, J, Sahl, SJ, and Hell, SW (2015) STED nanoscopy with fluorescent quantum dots. Nature Communications 6, 7127.

Harrison, MS, Hung, C-S, Liu, T-t, Christiano, R, Walther, TC, and Burd, CG (2014) A mechanism for retromer endosomal coat complex assembly with cargo. Proceedings of the National Academy of Sciences of the United States of America 111, 267-272.

Harterink, M, Port, F, Lorenowicz, MJ, McGough, IJ, Silhankova, M, Betist, MC, van Weering, JR, van Heesbeen, RG, Middelkoop, TC, Basler, K, et al. (2011) A SNX3-dependent retromer pathway mediates retrograde transport of the Wnt sorting receptor Wntless and is required for Wnt secretion. Nat Cell Biol 13, 914-923.

Hegedus, K., Takats, S., Boda, A., Jipa, A., Nagy, P., Varga, K., Kovacs, A.L., and Juhasz, G. (2016) The Ccz1-Mon1-Rab7 module and Rab5 control distinct steps of autophagy. Mol Biol Cell 27, 3132-3142.

Hierro, A, Gershlick, DC, Rojas, AL, and Bonifacino, JS (2015) Formation of Tubulovesicular Carriers from Endosomes and Their Fusion to the trans-Golgi Network. International review of cell and molecular biology 318, 159-202.

Hill, E, van der Kaay, J, Downes, CP, and Smythe, E. (2001) The Role of Dynamin and Its Binding Partners in Coated Pit Invagination and Scission. The Journal of Cell Biology 152, 309-324.

Hirata, T, Fujita, M, Nakamura, S, Gotoh, K, Motooka, D, Murakami, Y, Maeda, Y, and Kinoshita, T (2015) Post-Golgi anterograde transport requires GARP-dependent endosome-to-TGN retrograde transport. Mol Biol Cell 26, 3071-3084.

Hong, W, and Lev, S (2014) Tethering the assembly of SNARE complexes. Trends in cell biology 24, 35-43.

Hong, Z, Yang, Y, Zhang, C, Niu, Y, Li, K, Zhao, X, and Liu, JJ (2009) The retromer component SNX6 interacts with dynactin p150(Glued) and mediates endosome-to-TGN transport. Cell Res 19, 1334-1349.

Horazdovsky, BF, Davies, BA, Seaman, MN, McLaughlin, SA, Yoon, S, and Emr, SD (1997) A sorting nexin-1 homologue, Vps5p, forms a complex with Vps17p and is required for recycling the vacuolar protein-sorting receptor. Mol Biol Cell 8, 1529-1541.

Hunt, SD, and Stephens, DJ (2011) The role of motor proteins in endosomal sorting. Biochem Soc Trans 39, 1179-1184.

Hunt, SD, Townley, AK, Danson, CM, Cullen, PJ, and Stephens, DJ (2013) Microtubule motors mediate endosomal sorting by maintaining functional domain organization. J Cell Sci 126, 2493-2501.

Hutagalung, AH, and Novick, PJ (2011) Role of Rab GTPases in Membrane Traffic and Cell Physiology. Physiological reviews 91, 119-149.

Irannejad, R, Kotowski, SJ, and von Zastrow, M (2014) Investigating signaling consequences of GPCR trafficking in the endocytic pathway. Methods in enzymology 535, 403-418.

Ishii, M, Suda, Y, Kurokawa, K, and Nakano, A (2016) COPI is essential for Golgi cisternal maturation and dynamics. Journal of Cell Science 129, 3251-3261.

Jia, D, Gomez, TS, Billadeau, DD, and Rosen, MK (2012) Multiple repeat elements within the FAM21 tail link the WASH actin regulatory complex to the retromer. Molecular Biology of the Cell 23, 2352-2361.

Kawamura, S, Nagano, M, Toshima, JY, and Toshima, J (2014) Analysis of subcellular localization and function of the yeast Rab6 homologue, Ypt6p, using a novel amino-terminal tagging strategy. Biochem Biophys Res Commun 450, 519-525.

Klinger, SC, Siupka, P, and Nielsen, MS (2015) Retromer-Mediated Trafficking of Transmembrane Receptors and Transporters. Membranes 5, 288-306.

Koumandou, VL, Klute, MJ, Herman, EK, Nunez-Miguel, R, Dacks, JB, and Field, MC (2011) Evolutionary reconstruction of the retromer complex and its function in Trypanosoma brucei. Journal of Cell Science 124, 1496-1509.

Krämer, L, and Ungermann, C (2011) HOPS drives vacuole fusion by binding the vacuolar SNARE complex and the Vam7 PX domain via two distinct sites. Molecular Biology of the Cell 22, 2601-2611.

Krueger, EW, Orth, JD, Cao, H, and McNiven, MA (2003) A dynamin-cortactin-Arp2/3 complex mediates actin reorganization in growth factor-stimulated cells. Mol Biol Cell 14, 1085-1096.

Kulkarni, A, Alpadi, K, Sirupangi, T, and Peters, C (2014) A dynamin homolog promotes the transition from hemifusion to content mixing in intracellular membrane fusion. Traffic (Copenhagen, Denmark) 15, 558-571.

Lall, P, Lindsay, AJ, Hanscom, S, Kecman, T, Taglauer, ES, McVeigh, UM, Franklin, E, McCaffrey, MW, and Khan, AR (2015) Structure-Function Analyses of the Interactions between Rab11 and Rab14 Small GTPases with Their Shared Effector Rab Coupling Protein (RCP) J Biol Chem 290, 18817-18832.

Lee, J, Retamal, C, Cuitiño, L, Caruano-Yzermans, A, Shin, J-E, van Kerkhof, P, Marzolo, M-P, and Bu, G (2008) Adaptor Protein Sorting Nexin 17 Regulates Amyloid Precursor Protein Trafficking and Processing in the Early Endosomes. The Journal of Biological Chemistry 283, 11501-11508.

Lees, JA, Yip, CK, Walz, T, and Hughson, FM (2010) Molecular organization of the COG vesicle tethering complex. Nature structural and molecular biology 17, 1292-1297.

Lerman, JC, Robblee, J, Fairman, R, and Hughson, FM (2000) Structural Analysis of the Neuronal SNARE Protein Syntaxin-1A. Biochemistry 39, 8470-8479.

Li, F, Yi, L, Zhao, L, Itzen, A, Goody, RS, and Wu, Y-W (2014) The role of the hypervariable C-terminal domain in Rab GTPases membrane targeting. Proceedings of the National Academy of Sciences of the United States of America 111, 2572-2577.

Liang, B, Kiessling, V, and Tamm, LK (2013) Prefusion structure of syntaxin-1A suggests pathway for folding into neuronal trans-SNARE complex fusion intermediate. Proceedings of the National Academy of Sciences of the United States of America 110, 19384-19389.

Lin, YC, Chiang, TC, Liu, YT, Tsai, YT, Jang, LT, and Lee, FJ (2011) ARL4A acts with GCC185 to modulate Golgi complex organization. J Cell Sci 124, 4014-4026.

Liu, JJ (2017) Regulation of dynein-dynactin-driven vesicular transport. Traffic 18, 336-347.

Liu, S, Majeed, W, Kudlyk, T, Lupashin, V, and Storrie, B (2016) Identification of Rab41/6d Effectors Provides an Explanation for the Differential Effects of Rab41/6d and Rab6a/a' on Golgi Organization. Frontiers in Cell and Developmental Biology 4.

Liu, YW, Lee, SW, and Lee, FJ (2006) Arl1p is involved in transport of the GPI-anchored protein Gas1p from the late Golgi to the plasma membrane. J Cell Sci 119, 3845-3855.

Llorente, A, Rapak, A, Schmid, SL, van Deurs, B, and Sandvig, K (1998) Expression of Mutant Dynamin Inhibits Toxicity and Transport of Endocytosed Ricin to the Golgi Apparatus. The Journal of Cell Biology 140, 553-563.

Lou, X, and Shin, YK (2016) SNARE zippering. Bioscience reports 36.

Lukehart, J, Highfill, C, and Kim, K (2013) Vps1, a recycling factor for the traffic from early endosome to the late Golgi. Biochemistry and cell biology = Biochimie et biologie cellulaire 91, 455-465.

Luo, L, Xue, J, Kwan, A, Gamsjaeger, R, Wielens, J, von Kleist, L, Cubeddu, L, Guo, Z, Stow, JL, Parker, MW, et al. (2016) The Binding of Syndapin SH3 Domain to Dynamin Proline-rich Domain Involves Short and Long Distance Elements. The Journal of biological chemistry 291, 9411-9424.

Luo, Z, and Gallwitz, D (2003) Biochemical and genetic evidence for the involvement of yeast Ypt6-GTPase in protein retrieval to different Golgi compartments. J Biol Chem 278, 791-799.

Lupashin, V, and Sztul, E (2005) Golgi tethering factors. Biochimica et Biophysica Acta (BBA) - Molecular Cell Research 1744, 325-339.

Ma, C, Li, W, Xu, Y, and Rizo, J (2011) Munc13 mediates the transition from the closed syntaxin–Munc18 complex to the SNARE complex. Nature structural and molecular biology 18, 542-549.

Ma, L, Kang, Y, Jiao, J, Rebane, AA, Cha, HK, Xi, Z, Qu, H, and Zhang, Y (2016) Alpha-SNAP Enhances SNARE Zippering by Stabilizing the SNARE Four-Helix Bundle. Cell reports 15, 531-539.

Malhotra, V, and Erlmann, P (2015) The pathway of collagen secretion. Annual review of cell and developmental biology 31, 109-124.

Mart, #xed, nez-Men, #xe1, rguez, J, #xe9, and A (2013) Intra-Golgi Transport: Roles for Vesicles, Tubules, and Cisternae. ISRN Cell Biology 2013, 15.

Mattila, JP, Shnyrova, AV, Sundborger, AC, Hortelano, ER, Fuhrmans, M, Neumann, S, Muller, M, Hinshaw, JE, Schmid, SL, and Frolov, VA (2015) A hemi-fission intermediate links two mechanistically distinct stages of membrane fission. Nature 524, 109-113.

McGough, IJ, Steinberg, F, Jia, D, Barbuti, PA, McMillan, KJ, Heesom, KJ, Whone, AL, Caldwell, MA, Billadeau, DD, Rosen, MK, et al. (2014) Retromer binding to FAM21 and the WASH complex is perturbed by the Parkinson disease-linked VPS35(D620N) mutation. Current biology : CB 24, 1670-1676.

Mehrotra, N, Nichols, J, and Ramachandran, R (2014) Alternate pleckstrin homology domain orientations regulate dynamin-catalyzed membrane fission. Molecular biology of the cell 25, 879-890.

Micaroni, M, Stanley, AC, Khromykh, T, Venturato, J, Wong, CX, Lim, JP, Marsh, BJ, Storrie, B, Gleeson, PA, and Stow, JL (2013) Rab6a/a' are important Golgi regulators of pro-inflammatory TNF secretion in macrophages. PloS one 8, e57034.

Miller, KE, Kim, Y, Huh, W-K, and Park, H-O (2015) Bimolecular fluorescence complementation (BiFC) analysis: advances and recent applications for genome-wide interaction studies. Journal of molecular biology 427, 2039-2055.

Miller, PM, Folkmann, AW, Maia, ARR, Efimova, N, Efimov, A, and Kaverina, I (2009) Golgi-derived CLASP-dependent Microtubules Control Golgi Organization and Polarized Trafficking in Motile Cells. Nature cell biology 11, 1069-1080.

Mirsafian, H, Mat Ripen, A, Merican, AF, and Bin Mohamad, S (2014) amino acid) sequence and structural comparison of BACE1 and BACE2 using evolutionary trace method. TheScientificWorldJournal 2014, 482463.

Mishra, R, Smaczynska-de Rooij, II, Goldberg, MW, and Ayscough, KR (2011) Expression of Vps1 I649K a self-assembly defective yeast dynamin, leads to formation of extended endocytic invaginations. Communicative and Integrative Biology 4, 115-117.

Morlot, S, Galli, V, Klein, M, Chiaruttini, N, Manzi, J, Humbert, F, Dinis, L, Lenz, M, Cappello, G, and Roux, A (2012) Membrane shape at the edge of the dynamin helix sets location and duration of the fission reaction. Cell 151, 619-629.

Morlot, S, and Roux, A (2013) Mechanics of Dynamin-Mediated Membrane Fission. Annual review of biophysics 42, 629-649.

Mukhopadhyay, S, and Linstedt, AD (2013) Retrograde trafficking of AB(5) toxins: mechanisms to therapeutics. Journal of molecular medicine (Berlin, Germany) 91, 1131-1141.

Murray, DH, Jahnel, M, Lauer, J, Avellaneda, MJ, Brouilly, N, Cezanne, A, Morales-Navarrete, H, Perini, ED, Ferguson, C, Lupas, AN, et al. (2016) An endosomal tether undergoes an entropic collapse to bring vesicles together. Nature 537, 107-111.

Oesterlin, LK, Goody, RS, and Itzen, A (2012) Posttranslational modifications of Rab proteins cause effective displacement of GDP dissociation inhibitor. Proc Natl Acad Sci U S A 109, 5621-5626.

Oka, T, Ungar, D, Hughson, FM, and Krieger, M (2004) The COG and COPI Complexes Interact to Control the Abundance of GEARs, a Subset of Golgi Integral Membrane Proteins. Molecular Biology of the Cell 15, 2423-2435.

Okada, H, Zhang, W, Peterhoff, C, Hwang, JC, Nixon, RA, Ryu, SH, and Kim, TW (2010) Proteomic identification of sorting nexin 6 as a negative regulator of BACE1-mediated APP processing. Faseb j 24, 2783-2794.

Orsel, JG, Sincock, PM, Krise, J, and Pfeffer, SR (2000) Recognition of the 300-kDa mannose 6-phosphate receptor cytoplasmic domain by 47-kDa tail-interacting protein. Proceedings of the National Academy of Sciences of the United States of America 97, 9047-9051.

Osterrieder, A (2012) Tales of tethers and tentacles: golgins in plants. Journal of microscopy 247, 68-77.

Panic, B, Whyte, JR, and Munro, S (2003) The ARF-like GTPases Arl1p and Arl3p act in a pathway that interacts with vesicle-tethering factors at the Golgi apparatus. Current biology : CB 13, 405-410.

Parlati, F, Varlamov, O, Paz, K, McNew, JA, Hurtado, D, Sollner, TH, and Rothman, JE (2002) Distinct SNARE complexes mediating membrane fusion in Golgi transport based on combinatorial specificity. Proc Natl Acad Sci U S A 99, 5424-5429.

Perez-Victoria, FJ, and Bonifacino, JS (2009) Dual roles of the mammalian GARP complex in tethering and SNARE complex assembly at the trans-golgi network. Mol Cell Biol 29, 5251-5263.

Perez-Victoria, FJ, Mardones, GA, and Bonifacino, JS (2008) Requirement of the human GARP complex for mannose 6-phosphate-receptor-dependent sorting of cathepsin D to lysosomes. Mol Biol Cell 19, 2350-2362.

Pérez-Victoria, FJ, Schindler, C, Magadán, JG, Mardones, GA, Delevoye, C, Romao, M, Raposo, G, and Bonifacino, JS (2010) Ang2/Fat-Free Is a Conserved Subunit of the Golgi-associated Retrograde Protein Complex. Molecular Biology of the Cell 21, 3386-3395.

Peters, C, Baars, TL, Buhler, S, and Mayer, A (2004) Mutual control of membrane fission and fusion proteins. Cell 119, 667-678.

Phillips, SA, Barr, VA, Haft, DH, Taylor, SI, and Haft, CR (2001) Identification and characterization of SNX15, a novel sorting nexin involved in protein trafficking. J Biol Chem 276, 5074-5084.

Priya, A, Kalaidzidis, IV, Kalaidzidis, Y, Lambright, D, and Datta, S (2015) Molecular insights into Rab7-mediated endosomal recruitment of core retromer: deciphering the role of Vps26 and Vps35. Traffic 16, 68-84.

Protopopov, V, Govindan, B, Novick, P, and Gerst, JE (1993) Homologs of the synaptobrevin/VAMP family of synaptic vesicle proteins function on the late secretory pathway in S. cerevisiae. Cell 74, 855-861.

Puthenveedu, MA, and Linstedt, AD (2001) Evidence that Golgi structure depends on a p115 activity that is independent of the vesicle tether components giantin and GM130. The Journal of Cell Biology 155, 227-238.

Radulescu, AE, Mukherjee, S, and Shields, D (2011) The Golgi protein p115 associates with gamma-tubulin and plays a role in Golgi structure and mitosis progression. J Biol Chem 286, 21915-21926.

Reddy, JV, Burguete, AS, Sridevi, K, Ganley, IG, Nottingham, RM, and Pfeffer, SR (2006) A functional role for the GCC185 golgin in mannose 6-phosphate receptor recycling. Mol Biol Cell 17, 4353-4363.

Revelo, NH, Kamin, D, Truckenbrodt, S, Wong, AB, Reuter-Jessen, K, Reisinger, E, Moser, T, and Rizzoli, SO (2014) A new probe for super-resolution imaging of membranes elucidates trafficking pathways. The Journal of Cell Biology 205, 591-606.

Rink, J, Ghigo, E, Kalaidzidis, Y, and Zerial, M (2005) Rab conversion as a mechanism of progression from early to late endosomes. Cell 122, 735-749.

Risselada, HJ, and Grubmüller, H (2012) How SNARE molecules mediate membrane fusion: Recent insights from molecular simulations. Current Opinion in Structural Biology 22, 187-196.

Rizo, J, and Xu, J (2013) Synaptic Vesicle Fusion without SNARE Transmembrane Regions. Developmental cell 27, 124-126.

Roberts, AJ, Kon, T, Knight, PJ, Sutoh, K, and Burgess, SA (2013) Functions and mechanics of dynein motor proteins. Nature reviews Molecular cell biology 14, 713-726.

Rooij, IIS-d, Allwood, EG, Aghamohammadzadeh, S, Hettema, EH, Goldberg, MW, and Ayscough, KR (2010) A role for the dynamin-like protein Vps1 during endocytosis in yeast. Journal of Cell Science 123, 3496-3506.

Ru, Hsia, Strong, J, Romano, J, Coppens, I, (2015) Studying Membrane Trafficking in Toxoplasma gondii Using Correlative Light and Electron Microscopy (CLEM) Microscopy Society of America 21, 2.

Ryder, PV, Vistein, R, Gokhale, A, Seaman, MN, Puthenveedu, MA, and Faundez, V (2013) The WASH complex, an endosomal Arp2/3 activator, interacts with the Hermansky–Pudlak syndrome complex BLOC-1 and its cargo phosphatidylinositol-4-kinase type IIα. Molecular Biology of the Cell 24, 2269-2284.

Saimani, U, Smothers, J, McDermott, H, Makaraci, P, and Kim, K (2017) Yeast dynamin associates with the GARP tethering complex for endosome-to-Golgi traffic. European journal of cell biology.

Sandvig, K, Skotland, T, van Deurs, B, and Klokk, TI (2013) Retrograde transport of protein toxins through the Golgi apparatus. Histochem Cell Biol 140, 317-326.

Scheper, W, and Hoozemans, JJM (2015) The unfolded protein response in neurodegenerative diseases: a neuropathological perspective. Acta Neuropathologica 130, 315-331.

Schindler, C, Chen, Y, Pu, J, Guo, X, and Bonifacino, JS (2015) EARP, a multisubunit tethering complex involved in endocytic recycling. Nature cell biology 17, 639-650.

Schuller, A, Kornblum, C, Deschauer, M, Vorgerd, M, Schrank, B, Mengel, E, Lukacs, Z, Glaser, D, Young, P, Plockinger, U, et al. (2013) [Diagnosis and therapy of late onset Pompe disease]. Der Nervenarzt 84, 1467-1472.

Scott, GK, Gu, F, Crump, CM, Thomas, L, Wan, L, Xiang, Y, and Thomas, G (2003) The phosphorylation state of an autoregulatory domain controls PACS-1-directed protein traffic. The EMBO Journal 22, 6234-6244.

Scott, K, Gadomski, T, Kozicz, T, and Morava, E (2014) Congenital disorders of glycosylation: new defects and still counting. Journal of inherited metabolic disease 37, 609-617.

Seaman, MN (2012) The retromer complex - endosomal protein recycling and beyond. J Cell Sci 125, 4693-4702.

Seaman, MN, McCaffery, JM, and Emr, SD (1998) A membrane coat complex essential for endosome-to-Golgi retrograde transport in yeast. J Cell Biol 142.

Seemann, J, Jokitalo, EJ, and Warren, G (2000) The role of the tethering proteins p115 and GM130 in transport through the Golgi apparatus in vivo. Mol Biol Cell 11, 635-645.

Sincock, PM, Ganley, IG, Krise, JP, Diederichs, S, Sivars, U, O'Connor, B, Ding, L, and Pfeffer, SR (2003) Self-assembly is important for TIP47 function in mannose 6-phosphate receptor transport. Traffic 4, 18-25.

.

Siniossoglou, S (2005) Affinity purification of Ypt6 effectors and identification of TMF/ARA160 as a Rab6 interactor. Methods in enzymology 403, 599-607.

Siniossoglou, S, and Pelham, HR (2001) An effector of Ypt6p binds the SNARE Tlg1p and mediates selective fusion of vesicles with late Golgi membranes. Embo j 20, 5991-5998.

Siniossoglou, S, and Pelham, HRB (2002) Vps51p Links the VFT Complex to the SNARE Tlg1p. Journal of Biological Chemistry 277, 48318-48324.

Smaczynska-de, R, II, Marklew, CJ, Allwood, EG, Palmer, SE, Booth, WI, Mishra, R, Goldberg, MW, and Ayscough, KR (2015) Phosphorylation Regulates the Endocytic Function of the Yeast Dynamin-Related Protein Vps1. Mol Cell Biol 36, 742-755.

Smaczynska-de Rooij, II, Marklew, CJ, Allwood, EG, Palmer, SE, Booth, WI, Mishra, R, Goldberg, MW, and Ayscough, KR (2016) Phosphorylation Regulates the Endocytic Function of the Yeast Dynamin-Related Protein Vps1. Molecular and Cellular Biology 36, 742-755.

Smirnova, E, Shurland, DL, Newman-Smith, ED, Pishvaee, B, and van der Bliek, AM (1999) A model for dynamin self-assembly based on binding between three different protein domains. J Biol Chem 274, 14942-14947.

Smith, RD, and Lupashin, VV (2008) Role of the conserved oligomeric Golgi (COG) complex in protein glycosylation. Carbohydrate research 343, 2024-2031.

Sohda, M, Misumi, Y, Yamamoto, A, Nakamura, N, Ogata, S, Sakisaka, S, Hirose, S, Ikehara, Y, and Oda, K (2010) Interaction of Golgin-84 with the COG complex mediates the intra-Golgi retrograde transport. Traffic 11, 1552-1566.

Spang, A (2016) Membrane Tethering Complexes in the Endosomal System. Front Cell Dev Biol 4, 35.

Stein, IS, Gottfried, A, Zimmermann, J, and Fischer von Mollard, G (2009) TVP23 interacts genetically with the yeast SNARE VTI1 and functions in retrograde transport from the early endosome to the late Golgi. The Biochemical journal 419, 229-236.

Stein, M, Pilli, M, Bernauer, S, Habermann, BH, Zerial, M, and Wade, RC (2012) The interaction properties of the human Rab GTPase family--comparative analysis reveals determinants of molecular binding selectivity. PloS one 7, e34870.

Suda, Y, Kurokawa, K, Hirata, R, and Nakano, A (2013a) Rab GAP cascade regulates dynamics of Ypt6 in the Golgi traffic. Proc Natl Acad Sci U S A 110, 18976-18981.

Suda, Y, and Nakano, A (2012) The yeast Golgi apparatus. Traffic (Copenhagen, Denmark) 13, 505-510.

Sundborger, AC, Fang, S, Heymann, JA, Ray, P, Chappie, JS, and Hinshaw, JE (2014) A dynamin mutant defines a super-constricted pre-fission state. Cell reports 8, 734-742.

Suvorova, ES, Duden, R, and Lupashin, VV (2002) The Sec34/Sec35p complex, a Ypt1p effector required for retrograde intra-Golgi trafficking, interacts with Golgi SNAREs and COPI vesicle coat proteins. J Cell Biol 157, 631-643.

Südhof, TC, and Rizo, J (2011) Synaptic vesicle exocytosis. Cold Spring Harbor perspectives in biology 3, 10.1101/cshperspect.a005637 a005637.

Swaney, DL, Beltrao, P, Starita, L, Guo, A, Rush, J, Fields, S, Krogan, NJ, and Villen, J (2013) Global analysis of phosphorylation and ubiquitylation cross-talk in protein degradation. Nature methods 10, 676-682.

Swarbrick, JD, Shaw, DJ, Chhabra, S, Ghai, R, Valkov, E, Norwood, SJ, Seaman, M.N., and Collins, B.M. (2011) VPS29 is not an active metallo-phosphatase but is a rigid scaffold required for retromer interaction with accessory proteins. PloS one 6, e20420.

Tani, M, and Kuge, O (2012) Involvement of complex sphingolipids and phosphatidylserine in endosomal trafficking in yeast Saccharomyces cerevisiae. Molecular microbiology 86, 1262-1280.

Thomas, LL, and Fromme, JC (2016) GTPase cross talk regulates TRAPPII activation of Rab11 homologues during vesicle biogenesis. J Cell Biol 215, 499-513.

Trahey, M, and Hay, JC (2010) Transport vesicle uncoating: it's later than you think. F1000 Biology Reports 2, 47.

Trousdale, CM, Goud Gadila S, Saimani U, Kim K (2017) The Functional Relationship between the Retromer and Yeast Dynamin at the Endosome. THE INTERNATIONAL JOURNAL OF SCIENCE and TECHNOLEDGE.

Ungermann, C, and Langosch, D (2005) Functions of SNAREs in intracellular membrane fusion and lipid bilayer mixing. J Cell Sci 118, 3819-3828.

Valenzuela, JI, and Perez, F (2015) Diversifying the secretory routes in neurons. Frontiers in Neuroscience 9, 358.

van Weering, JR, Brown, E, Sharp, TH, Mantell, J, Cullen, PJ, and Verkade, P (2010) Intracellular membrane traffic at high resolution. Methods in cell biology 96, 619-648.

van Weering, JR, Verkade, P, and Cullen, PJ (2012) SNX-BAR-mediated endosome tubulation is co-ordinated with endosome maturation. Traffic 13, 94-107.

Vilarino-Guell, C, Wider, C, Ross, OA, Dachsel, JC, Kachergus, JM, Lincoln, SJ, Soto-Ortolaza, AI, Cobb, SA, Wilhoite, GJ, Bacon, JA, et al. (2011) VPS35 mutations in Parkinson disease. American journal of human genetics 89, 162-167.

Wandinger-Ness, A, and Zerial, M (2014) Rab Proteins and the Compartmentalization of the Endosomal System. Cold Spring Harbor perspectives in biology 6, a022616.

Wang, F, Zhang, L, Zhang, G-L, Wang, Z-B, Cui, X-S, Kim, N-H, and Sun, S-C (2014) WASH complex regulates Arp2/3 complex for actin-based polar body extrusion in mouse oocytes. Scientific Reports 4, 5596.

Wendler, F, and Tooze, S (2001) Syntaxin 6: the promiscuous behaviour of a SNARE protein. Traffic 2, 606-611.

Weninger, K, Bowen, ME, Chu, S, and Brunger, AT (2003) Single-molecule studies of SNARE complex assembly reveal parallel and antiparallel configurations. Proc Natl Acad Sci U S A 100, 14800-14805.

Wesolowski, J, and Paumet, F (2010) SNARE motif: A common motif used by pathogens to manipulate membrane fusion. Virulence 1, 319-324.

Wiederhold, K, and Fasshauer, D (2009) Is Assembly of the SNARE Complex Enough to Fuel Membrane Fusion? The Journal of Biological Chemistry 284, 13143-13152.

Willett, R, Pokrovskaya, I, Kudlyk, T, and Lupashin, V (2014) Multipronged interaction of the COG complex with intracellular membranes. Cellular Logistics 4, e27888.

Williams, M, and Kim, K (2014) From membranes to organelles: emerging roles for dynamin-like proteins in diverse cellular processes. Eur J Cell Biol 93, 267-277.

Yang, S, and Rosenwald, AG (2016) Autophagy in Saccharomyces cerevisiae requires the monomeric GTP-binding proteins, Arl1 and Ypt6. Autophagy 12, 1721-1737.

Ye, X, and Cai, Q (2014) Snapin-Mediated BACE1 Retrograde Transport Is Essential for its Degradation in Lysosomes and Regulation of APP Processing in Neurons. Cell reports 6, 24-31.

Ye, X, Feng, T, Tammineni, P, Chang, Q, Jeong, YY, Margolis, DJ, Cai, H, Kusnecov, A, and Cai, Q (2017) Regulation of Synaptic Amyloid-beta Generation through BACE1 Retrograde Transport in a Mouse Model of Alzheimer's Disease. The Journal of neuroscience : the official j ournal of the Society for Neuroscience 37, 2639-2655.

Zhang, X, and Song, W (2013) The role of APP and BACE1 trafficking in APP processing and amyloid-β generation. Alzheimer's Research and Therapy 5, 46.

Zhu, J, Zhou, K, Hao, J-J, Liu, J, Smith, N, and Zhan, X (2005) Regulation of cortactin/dynamin interaction by actin polymerization during the fission of clathrin-coated pits. Journal of Cell Science 118, 807-817.

Zimprich, A, Benet-Pages, A, Struhal, W, Graf, E, Eck, SH, Offman, MN, Haubenberger, D, Spielberger, S, Schulte, EC, Lichtner, P, et al. (2011) A mutation in VPS35, encoding a subunit of the retromer complex, causes late-onset Parkinson disease. American journal of human genetics 89, 168-175.

Table 1. Yeast Strains Used in this Study

Strain	Source	Genotype
KKY 0002	Invitrogen	*MATa his3Δ1 leu2Δ0 met15Δ0 ura3Δ0*
KKY 0352	This study	*MATα his3Δura3Δleu2Δtrp1Δlys2Δ VPS1::KanMx6*
KKY 0811	This study	KKY 0002 *YPT6::HIS*
KKY 0995	This study	KKY 0352 *(pRS416-GFP-Snc1-PM)*
KKY 1004	This study	KKY 0002 *(pRS416-GFP-Snc1-PM)*
KKY 1254	Clontech	MATα, ura3-52, his3-200, ade2-101, trp1-901, leu2-3, 112, gal4Δ, gal80Δ, met-, URA3::$GAL1_{UAS}$-$Gal1_{TATA}$-LacZ, MEL1
KKY 1255	Clontech	MATa, trp1-901, leu2-3, 112, ura3-52, his3-200, gal4Δ, gal80Δ, LYS2::$GAL1_{UAS}$-$Gal1_{TATA}$-His3, $GAL2_{UAS}$-$Gal2_{TATA}$-Ade2 URA3::$MEL1_{UAS}$-$Mel1_{TATA}$ AUR1-C MEL1
KKY 1272	This study	KKY 1254 *(pGBKT7-LAM)*
KKY 1273	This study	KKY 1255 *(pGADT7-T)*
KKY 1274	This study	KKY 1254 *(pGBKT7-53)*
KKY 1275	This study	KKY 1254 (*pGBKT7-Vps1)*
KKY 1302	This study	KKY 1255 (*pGADT7-Ypt6)*
KKY 1304	This study	KKY 1274/KKY 1273 (diploid)
KKY 1305	This study	KKY 1272/KKY 1273 (diploid)
KKY 1419	This study	KKY 1302/KKY 1438 (diploid)
KKY 1420	This study	KKY 1302/KKY 1439 (diploid)

Table 1. Yeast Strains Used in this Study (Continued)

Strain	Source	Genotype
KKY 1421	This study	KKY 1302/KKY 1440 (diploid)
KKY 1438	This study	KKY 1254 (*pGBKT7-Vps1 (1-340 aa))*
KKY 1439	This study	KKY 1254 *(pGBKT7-Vps1 (341-614 aa))*
KKY 1440	This study	KKY 1254 *(pGBKT7-Vps1 (615-704 aa))*
KKY 1508	This study	KKY 1255 *(pGADT7-Vti1 (1-130 aa))*
KKY 1537	This study	KKY 1527 *(pcav29-vps1-ΔN)*
KKY 1539	This study	KKY 1527 *(pcav33- vps1-ΔC)*
KKY 1631	This study	KKY 1255 *(pGADT7-Ypt6 (1-72 aa))*
KKY 1632	This study	KKY 1255 *(pGADT7-Ypt6 (73-142 aa))*
KKY 1633	This study	KKY 1255 *(pGADT7-Ypt6 (143-215 aa))*
KKY 1642	This study	KKY 1275/ KKY 1631 (diploid)
KKY 1643	This study	KKY 1275/ KKY 1632 (diploid)
KKY 1644	This study	KKY 1275/ KKY 1633 (diploid)
KKY 1668	This study	KKY 1526 (*pCAV30-Vps1^{G315})*
KKY 1669	This study	KKY 1526 *(pCAV30-Vps1^{S43N})*

Table 1. Yeast Strains Used in this Study (Continued)

Strain	Source	Genotype
KKY 1690	This study	KKY 1440/KKY 1631 (diploid)
KKY 1691	This study	KKY 1438/KKY 1632 (diploid)
KKY 1692	This study	KKY 1439/KKY 1632 (diploid)
KKY 1693	This study	KKY 1440/KKY 1632 (diploid)
KKY 1694	This study	KKY 1438/KKY 1633 (diploid)
KKY 1695	This study	KKY 1439/KKY 1633 (diploid)
KKY 1696	This study	KKY 1440/KKY 1633 (diploid)
KKY 1699	This study	KKY 1255 *(pGADT7-Vti1 (1-186 aa))*
KKY 1701	This study	KKY 1527 (*pCAV30-Vps1^{G315})*
KKY 1702	This study	KKY 1527 *(pCAV30-Vps1^{S43N})*
KKY 1703	This study	KKY 1527 *(pCAV30-Vps1^{K42N})*
KKY 1704	This study	KKY 1527 *(pCAV30-Vps1)*
KKY 1715	This study	KKY 1255 *(pGADT7-Tlg2 (1-35 aa))*
KKY 1728	This study	KKY 1275/KKY 1715 (diploid)
KKY 1729	This study	KKY 1275/KKY 1700 (diploid)
KKY 1730	This study	KKY 1275/KKY 1699 (diploid)
KKY 1731	This study	KKY 1255 *(pGADT7-Tlg1 (1-131 aa))*
KKY 1747	This study	KKY 0352 *TRP::Vps10-GFP*

Table 1. Yeast Strains Used in this Study (Continued)

Strain	Source	Genotype
KKY 1751	This study	KKY 1275/KKY 1731 (diploid)
KKY 1826	This study	KKY 1255 *(pGADT7-Vti1 (130-186 aa))*
KKY 1827	This study	KKY 1255 *(pGADT7-Snc2 (1-52 aa))*
KKY 1828	This study	KKY 1255 *(pGADT7-Snc2 (52-96 aa))*
KKY 1829	This study	KKY 1255 *(pGADT7-Snc2 (28-96 aa))*
KKY 1859	This study	KKY 0811 *(P_{TPI1}-GFP-SNC1pm)*
KKY 1864	This study	KKY 0352 *(p416-TEF-mRFP-Ypt6)*
KKY 1868	This study	KKY 1275/KKY 1508 (diploid)
KKY 1869	This study	KKY 1275/KKY 1826 (diploid)
KKY 1870	This study	KKY 1275/KKY 1827 (diploid)
KKY 1871	This study	KKY 1275/KKY 1828 (diploid)
KKY 1872	This study	KKY 1275/KKY 1829 (diploid)
KKY 1873	This study	KKY 1747 *(pCAV30-Vps1^{K42N})*
KKY 1874	This study	KKY 1747 *(pCAV30-Vps1^{S43N})*
KKY 1875	This study	KKY 1747 (*pCAV30-Vps1^{G315})*
KKY 1886	This study	KKY 0002 *TRP::Vps10-GFP*

Table 2. Bacterial Plasmids Used in this Study

Plasmid	Source	Plasmid Name
KKD 0007	(Longtine et al., 1998)	pFA6a-GFP (S65T)-TRP1
KKD 0062	(Furuta et al., 2007)	P_{TPI1}-GFP-SNC1pm URA3 CEN
KKD 0064	(Furuta et al., 2007)	P_{TPI1}-GFP-SNC1 URA3 CEN
KKD 0079	This study	pGBKT7-Vps1
KKD 0082	This study	pGADT7-Ypt6
KKD 0083	Clontech	pGADT7
KKD 0089	(Vater et al., 1992)	pCAV29-*vps1*-Δ*N*
KKD 0090	(Vater et al., 1992)	pCAV30-Vps1
KKD 0092	(Vater et al., 1992)	pCAV33- *vps1*-Δ*C*
KKD 0099	Clontech	pGBKT7
KKD 0129	(Goud Gadila et al., 2017)	pGBKT7-Vps1 (341-614 aa)
KKD 0130	(Goud Gadila et al., 2017)	pGBKT7-Vps1 (615-704 aa)
KKD 0134	(Goud Gadila et al., 2017)	pGBKT7- Vps1 (1-340 aa)
KKD 0143	(Obara et al., 2013)	pOK489 (mRFP-Cps1)
KKD 0174	This study	pGADT7-Ypt6^{G139E}
KKD 0187	This study	pGADT7-Tlg1 (1-131 aa)
KKD 0251	This study	pGADT7-Ypt6^{T24N}
KKD 0252	This study	pGADT7-Ypt6^{Q69L}
KKD 0271	This study	pGADT7-Ypt6 (1-72 aa)
KKD 0272	This study	pGADT7-Ypt6 (73-142 aa)
KKD 0273	This study	pGADT7-Ypt6 (143-215 aa)

Table 2. Bacterial Plasmids Used in this Study (continued)

Plasmid	Source	Plasmid Name
KKD 0274	This study	pCAV-Vps1^{G315D}
KKD 0275	This study	pCAV-Vps1^{S43N}
KKD 0276	This study	pCAV-Vps1^{K42E}
KKD 0309	This study	pGADT7-Vti1 (1-186 aa)
KKD 0311	This study	pGADT7-Snc2 (1-96 aa)
KKD 0313	This study	pGADT7-Tlg2 (1-35 aa)
KKD 0315	This study	p416-TEF-mRFP-Ypt6
KKD 0323	This study	pGADT7-Vti1 (1-130 aa)
KKD 0324	This study	pGADT7-Vti1 (130-186 aa)
KKD 0325	This study	pGADT7-Snc2 (1-52 aa)
KKD 0326	This study	pGADT7-Snc2 (28-96 aa)
KKD 0327	This study	pGADT7-Snc2 (52-96 aa)

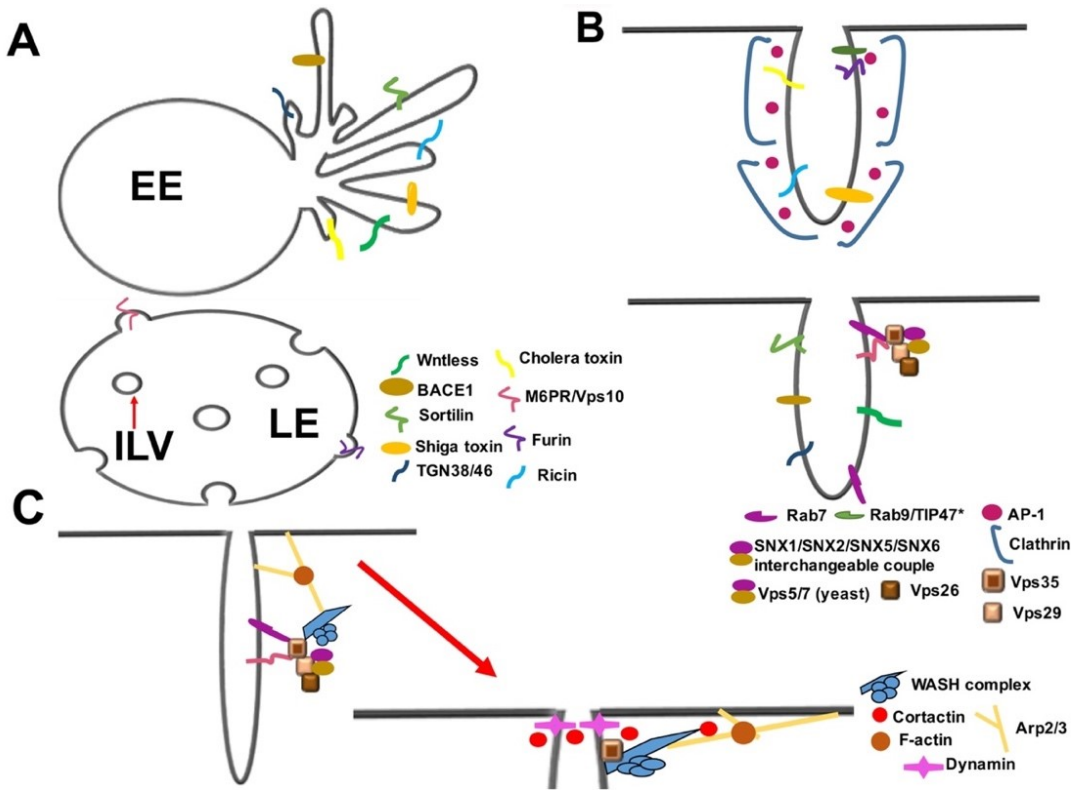

Figure 1. A schematic diagram for the endosome-to-TGN retrograde trafficking. **A)** Representative transport cargo from the early (EE) and late endosome (LE). Many projected tubules emerging from the EE present a diverse range of cargo and act as a cargo sorting station for the retrograde pathway (Burd, 2011). Maturation of the EE leads to the continuum to the LE that carries intraluminal vesicles (ILVs). Cargo including but not limited to, Wntless, BACE1, Sortilin, Shiga toxin, TGN 38/46, Ricin, and Cholera toxin, leave the EE, whereas M6PR/Vps10 and furin are transported from the LE via endosome-derived vesicles to the TGN (Harterink et al., 2011; Klinger et al., 2015; Mirsafian et al., 2014). **B)** Mechanisms of invagination and coating of an emerging transport vesicle. A wide range of cargo is coated by clathrin or the retromer complex. For example, clathrin coats the surface of vesicles containing Shiga toxin, ricin, Cholera toxin, and furin. The sorting of Wntless, BACE1, Sortilin, TGN 38/46, and M6PR/Vps10 is assisted by the interaction with the retromer complex (Burd and Cullen, 2014; Sandvig et al., 2013). Even though coating proteins are crucial for the cargo selection and sorting, furin additionally requires Rab9 GTPase to be transferred to the TGN, whereas M6PRs are TIP47-dependent (Chia et al., 2011). **C)** Elongation and fission of a vesicle pit. The WASH complex, a nucleation-promoting factor, localizes at endosomes to stimulate the Arp2/3 complex-mediated actin polymerization for vesicle fission (Ryder et al., 2013). Cortactin collaborates with the WASH complex not only to promote actin polymerization and stabilization but also to recruit dynamin to the fission site (Derivery et al., 2012; Derivery et al., 2009; Eiseler et al., 2010; Krueger et al., 2003) Dynamin dimers assemble around the neck of the invaginated vesicle neck, constricting the neck of the vesicle and forcing the vesicle to be pinched off from endosomal membranes (Chi et al., 2014).

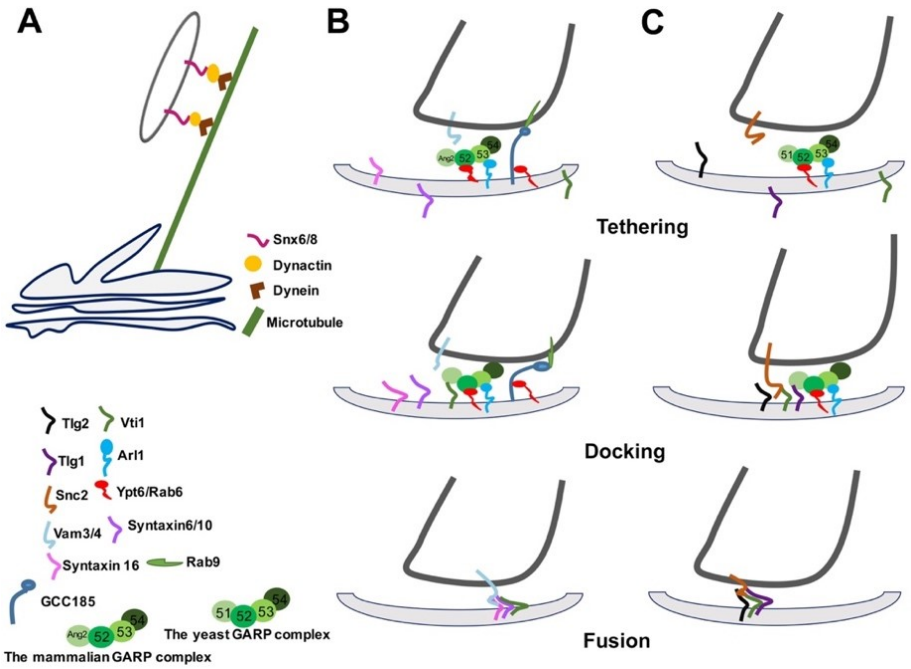

Figure 2. The endosome-derived vesicle movement towards the TGN. **A)** The freed endosome-derived vesicle travels toward the TGN. The retromer-dependent vesicle trafficking to the TGN requires Snx6, whereas Snx8 contributes to the retromer-independent vesicle traveling towards the TGN (Hong et al., 2009). Snx6 has been demonstrated to interact with dynactin, which bridges the vesicle to the dynein-associated microtubules (Hunt et al., 2013). However, Snx8 interacts with dynein directly (Hunt et al., 2013). Dynein regulates sliding of the endosome-derived vesicle on microtubules t (Roberts et al., 2013). **B)** Endosome-derived vesicle tethering/fusion to the TGN in mammalian cells. Small GTPases including Rab6 and Arl1 play a role in the recruitment of the GARP to the TGN through their interaction with Vps52 and Vps53, respectively (Benjamin et al., 2011). It is suggested that the binding of Vps52 to Rab6 triggers the recruitment of other subunits, Ang2, Vps52, and Vps54 to the TGN membranes. A Rab9 GTPase carrying vesicle derived from the LE is recognized and captured by GCC185, a TGN golgin. Then, GCC185 bends onto the TGN membrane, allowing the vesicle to come closer proximity of the TGN (Brown et al., 2011; Cheung et al., 2015; Cheung and Pfeffer, 2016). Tethering of the vesicle leads to its docking/fusion with the help of SNAREs that form a *trans*-SNARE complex. If the vesicle is originated from the early endosome, syntaxin 16/Vti1a/syntaxin 6/VAMP4 SNAREs bundle into the *trans*-SNARE complex. On the other hand, if the vesicle is traveling from the late endosome, syntaxin 16/Vti1a/ syntaxin 10/VAMP3 SNAREs participate in the formation of the *trans*-SNARE complex (Perez-Victoria and Bonifacino, 2009; Suda et al., 2013). The bundling of the *trans*-SNARE complex lead to a zippering event between two opposite membranes, which overcomes the fusion energy barriers of two opposite membranes. **C)** Tethering/fusion of the endosome-derived vesicle at the TGN in yeast cells. Rab6 homologue Ypt6 manages the process of the GARP complex (Vps51/Vps52/Vps53/Vps54) recruitment to the TGN (Perez-Victoria et al., 2008). The *trans*-SNARE complex is formed by Vti1, Tlg1, Tlg2 and Snc2 SNAREs to facilitate the endosome-derived vesicle fusion to the TGN (Furuta et al., 2007).

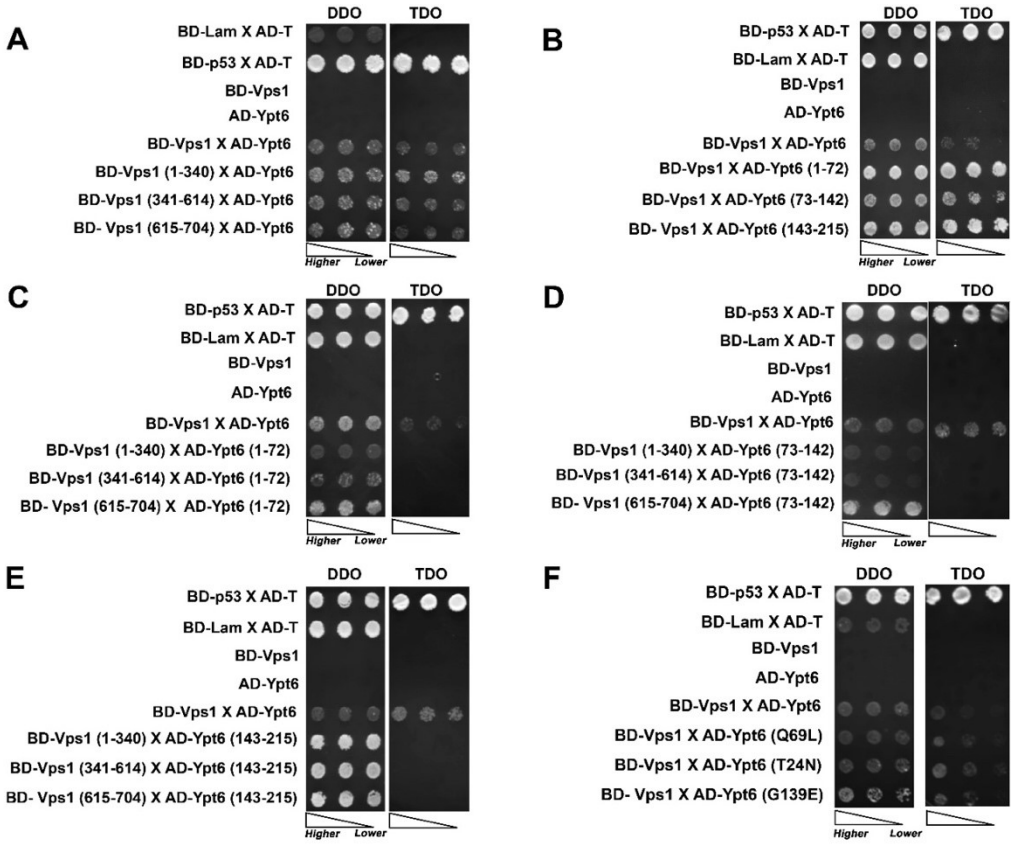

Figure 3. Vps1 interaction with Ypt6. **A)** Interaction of Vps1 and three domains of Vps1 with Ypt6. The positive control strain (KKY 1304) coexpresses BD-p53 and AD-T (AD-SV40 Large T antigen). The negative control strain (KKY 1305) coexpresses BD-Lam (BD-Lamin) and AD-T, not interacting with one another. Cells that express either AD-Ypt6 (KKY 1302) or BD-Vps1 (KKY 1275) were also used as negative controls. Three strains (KKY 1419, KKY 1420, and KKY 1421) were engineered to coexpress AD-Ypt6 and a BD-Vps1^{GTPase} (1-340aa), BD-Vps1^{Middle} (341-614aa), or BD-Vps1^{GED} (615-704aa) domain, respectively. A spotting assay was performed by serially diluting these yeast strains by a factor of 3, followed by plating the cells on selective media, such as DDO and TDO. Cell concentration gradients are indicated by triangles with the tip pointing toward the lower concentration. **B)** Mapping regions of Ypt6 that interacts with Vps1. Diploid strains (KKY 1642-1644) coexpressing BD-Vps1 and an indicated AD-fused Ypt6 fragment (Ypt6 1-72aa, Ypt6 73-142aa, or Ypt6 143-215aa) were subjected to a spotting assay described above. **C)** The AD-Ypt6 (1-72aa) fragment does not bind to any Vps1 (Vps1^{GTPase}, Vps1^{Middle}, or Vps1^{GED}) domain. **D)** No interaction of Vps1 domains (Vps1^{GTPase}, Vps1^{Middle}, or Vps1^{GED}) with AD-Ypt6 (73-142aa) was observed. **E)** The C-terminal one-third of Ypt6 (143-215aa) fragment does not bind to 3 different Vps1 domains. **F)** Vps1 interacts with both constitutively active (*ypt6*^{Q69L}) and inactive (*ypt6*^{T24N} and *ypt6*^{G139E}) Ypt6 mutants.

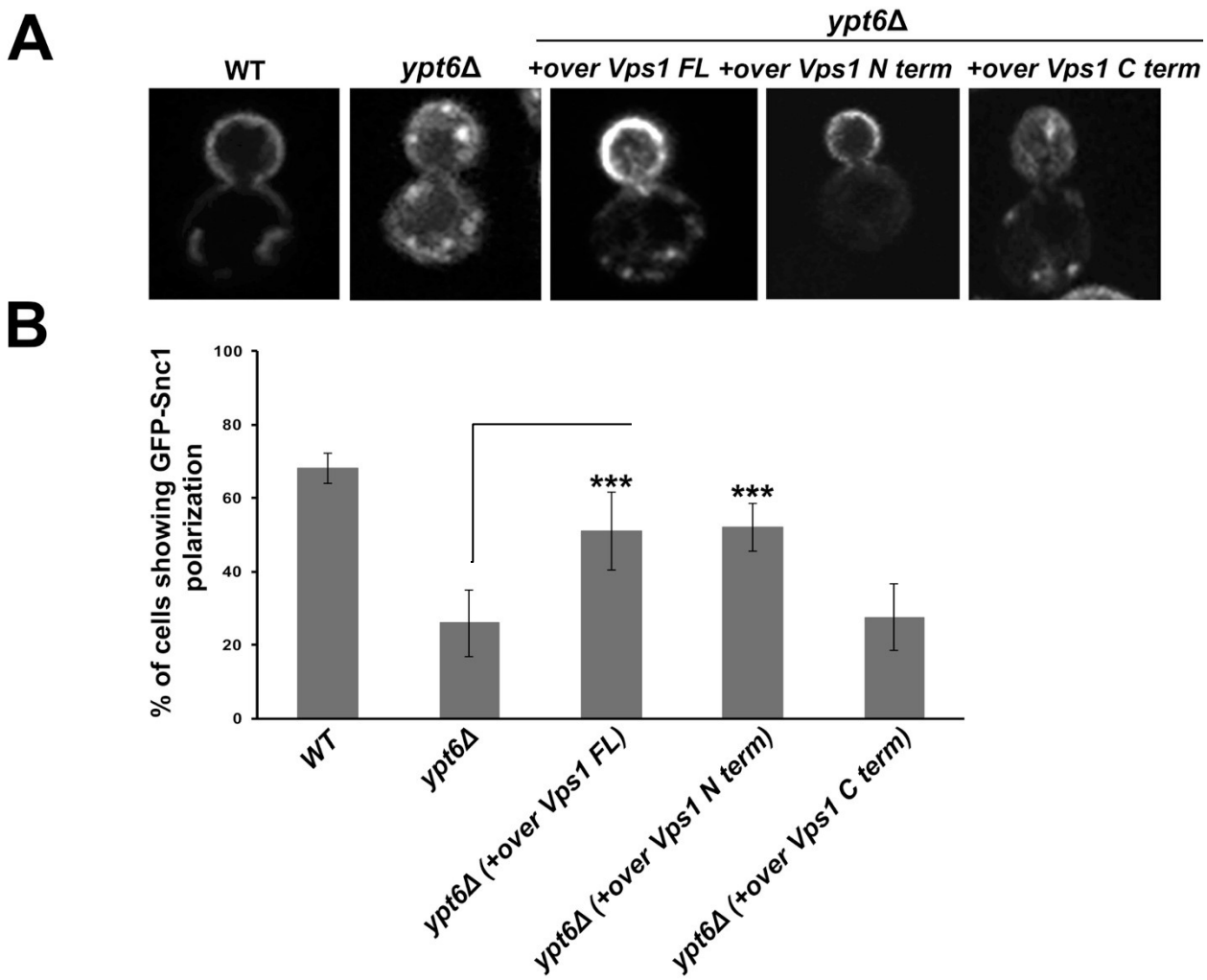

Figure 4. Effect of Vps1 overexpression on GFP-Snc1 polarization in a *ypt6*Δ strain **A)** Representative pictures of exogenously expressed GFP-Snc1 in WT (KKY 1525), *ypt6*Δ (KKY 1527), and *ypt6*Δ background cells overexpressing Vps1 full-length (KKY 1535), Vps1 N-terminal (KKY 1537), and Vps1 C-terminal (KKY 1539). **B)** Overexpression of Vps1 full-length and N-terminal Vps1 restore the defective GFP-Snc1 phenotype caused by *ypt6*Δ. The polarized appearance of GFP-Snc1 that was found at the bud plasma membrane was determined as the proper targeting of GFP-Snc1 (n=30 for each strain). The average of three data sets was calculated, and the student's *T*-test was performed using Microsoft Excel program. Three asterisks indicate *p*-value being smaller than 0.01.

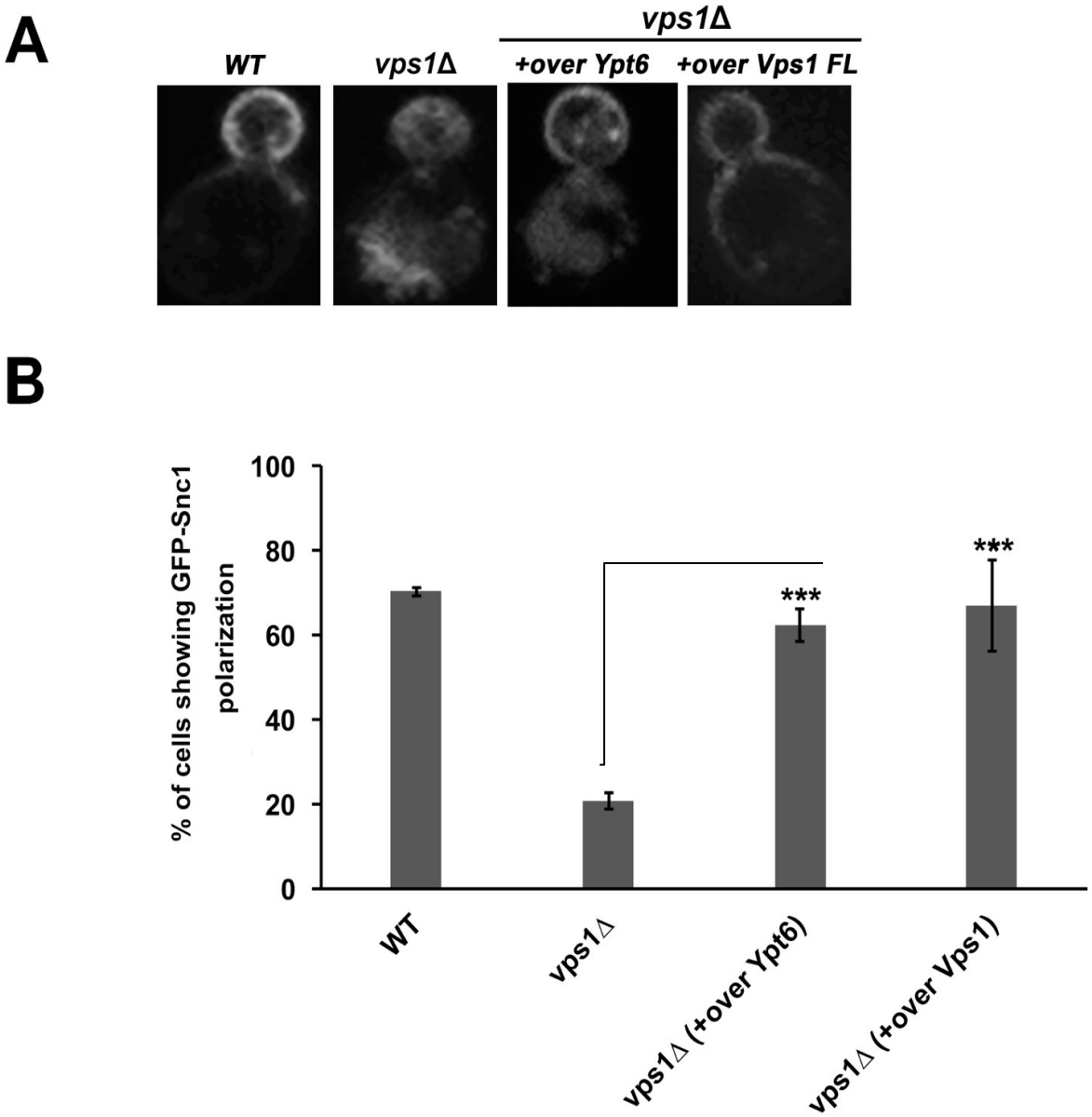

Figure 5. Overexpression of Ypt6 and Vps1 recovered the aberrant GFP-Snc1 phenotype caused by *vps1*Δ. **A)** GFP-Snc1 was exogenously expressed in WT (KKY 1525), *vps1*Δ (KKY 1526) strains. Additionally, KKY 1526 strain was used to overexpress Ypt6 (KKY 1859) and Vps1 (KKY 1529). Representative pictures are shown. **B)** Ypt6 overexpression increases the levels of GFP-Snc1 polarization in a *vps1*Δ strain. The confocal microscope images of GFP-Snc1 expressing strains were visualized. The average of three trials was quantified (n=30 for each strain). The *P* value less than ≤ 0.01 is indicated with three asterisks.

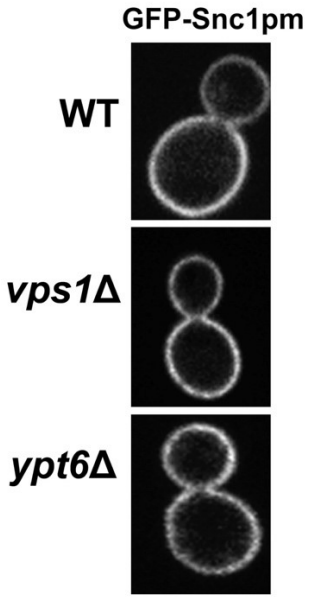

Figure 6. The defect in Snc1 recycling in cells lacking Ypt6 or Vps1 is not due to secretion abnormality. An endocytosis-defective mutant of GFP-Snc1 was expressed in WT (KKY 1004), *vps1*Δ (KKY 0995), and *ypt6*Δ (KKY 1860) cells.

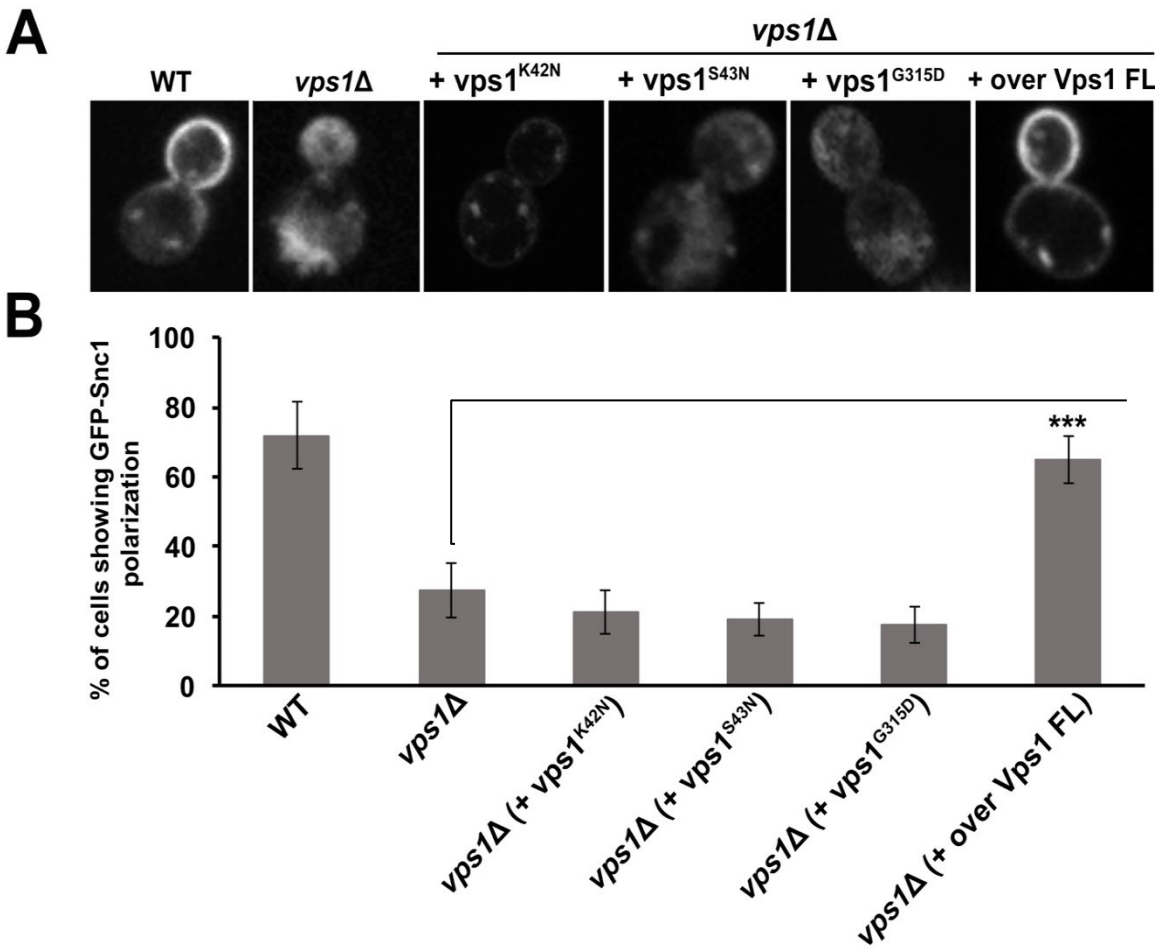

Figure 7. GTPase activity is required for Vps1 to rescue abnormal Snc1 recycling in *vps1*Δ cells. **A)** Representative pictures of GFP-Snc1-*vps1*Δ cells overexpressing Vps1 GTPase mutants. $vps1^{K42N}$, $vps1^{S43N}$, $vps1^{G315D}$, and Vps1 full-length were introduced into GFP-Snc1-*vps1*Δ cells (KKY 1668-1671, respectively). **B)** Vps1 GTPase mutants, $vps1^{K42N}$, $vps1^{S43N}$, or $vps1^{G315D}$ did not rescue GFP-Snc1 polarization in *vps1*Δ cells. Polarization levels of GFP-Snc1 were quantified in KKY 1668-1671 strains (three-trials, n=30). The *P* value less than ≤ 0.01 is indicated with three asterisks.

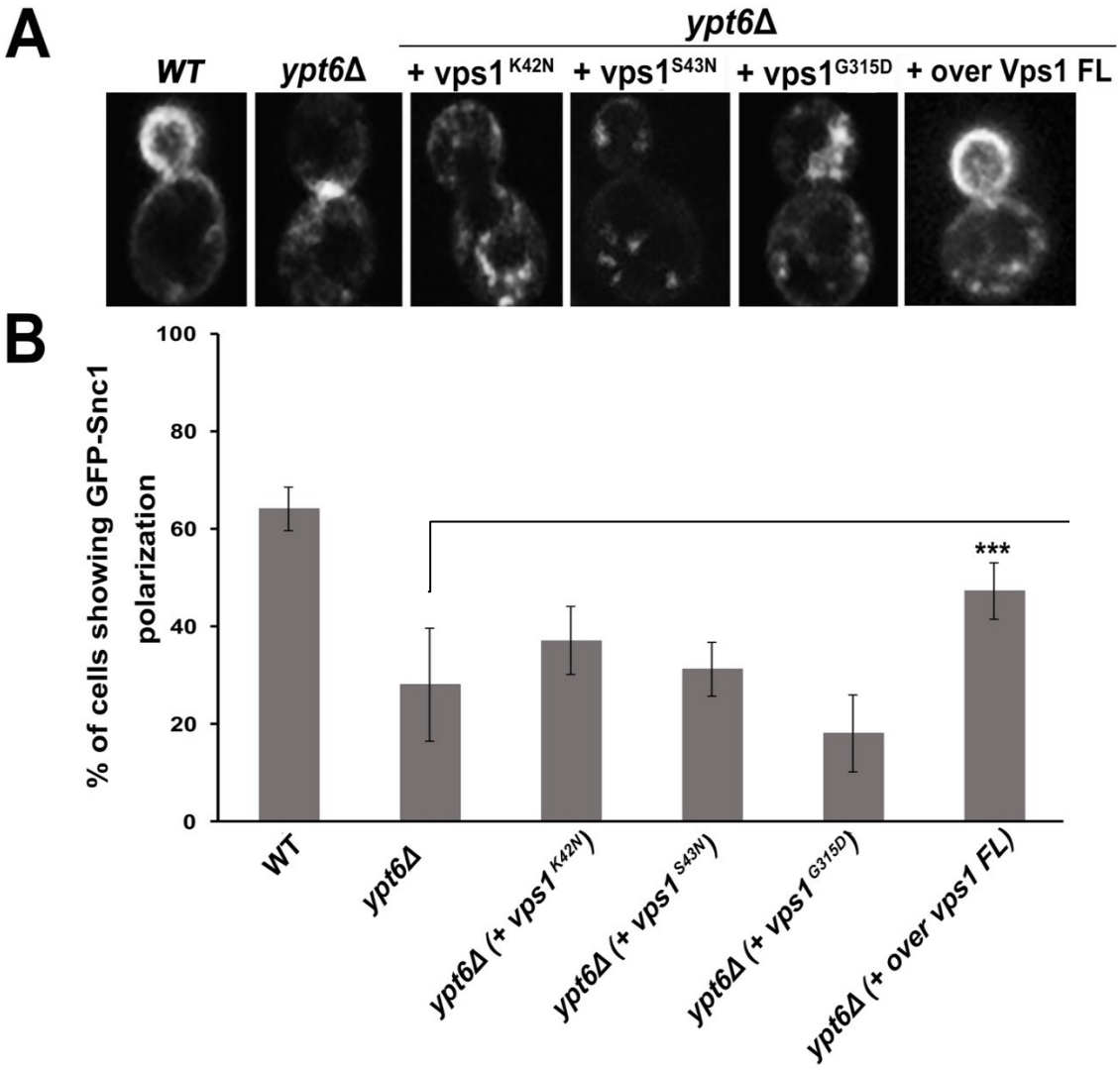

Figure 8. Vps1 GTPase activity is required for Vps1 to recover deficiencies in GFP-Snc1 polarization caused by *ypt6*Δ. **A)** Representative images of WT (KKY 1525), *ypt6*Δ (KKY 1527) and *ypt6*Δ overexpressing $vps1^{K42N}$, $vps1^{S43N}$, $vps1^{G315D}$ or Vps1 full-length (KKY 1701-1704) cells that exogenously express GFP-Snc1. **B)** Vps1 GTP-binding activity is essential for the polarized distribution of GFP-Snc1.Levels of GFP-Snc1 polarization in the strains described above was quantified in three different trials (n=30 for each strain). The *P* value less than ≤ 0.01 is indicated with three asterisks.

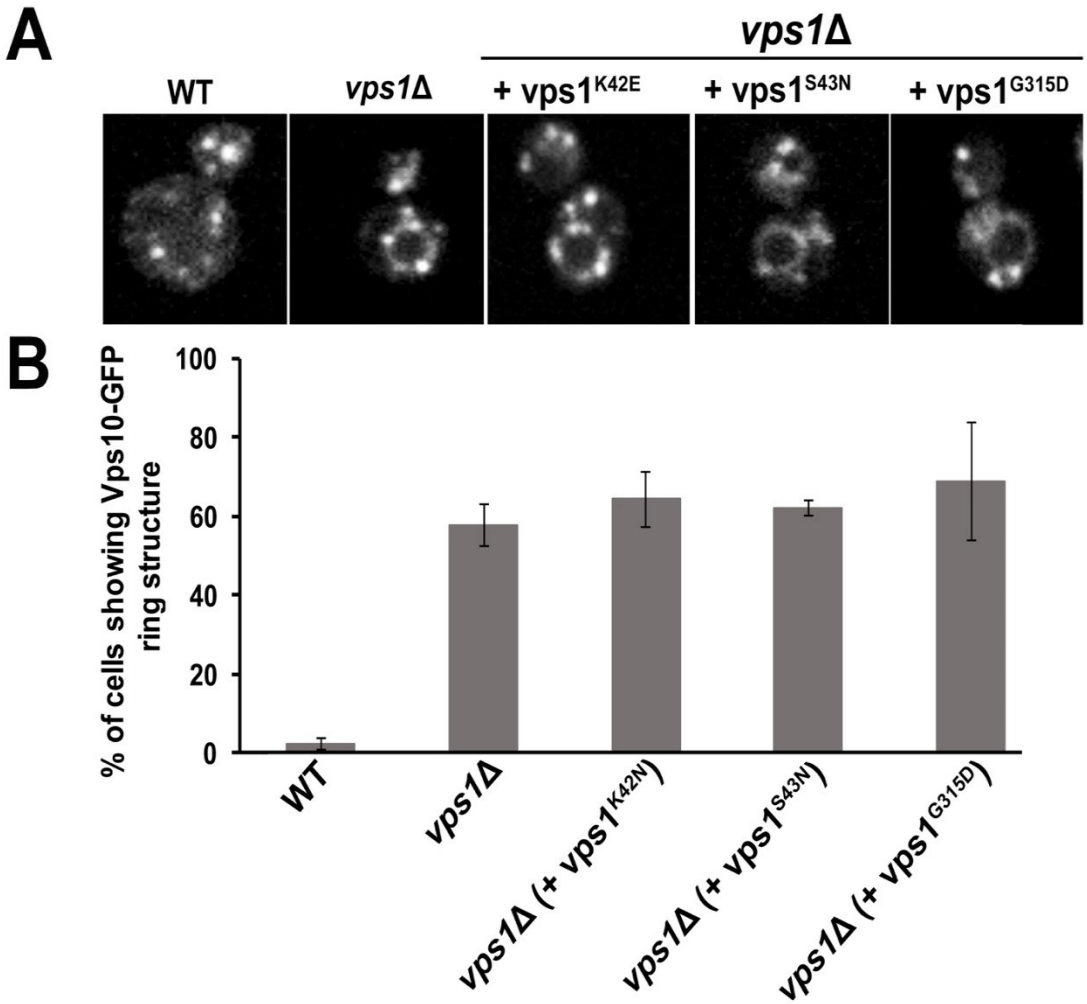

Figure 9. Vps1 is crucial for Vps10-GFP trafficking in the cells. **A)** Representative images of genomically tagged Vps10-GFP WT (KKY 1886), *vps1*Δ (KKY 1747), and *vps1*Δ cells that also express Vps1 GTPase mutant strains. **B)** The number of cells forming the cytosolic ring-like structure of Vps10-GFP puncta was significantly higher in cells lacking Vps1 and overexpressing $vps1^{K42N}$ (KKY 1875), $vps1^{S43N}$ (KKY 1874), or $vps1^{G315D}$ (KKY 1873). In three different data set, ring forming cells were marked down as it indicates GFP-Vps10 localization to the vacuole (n=30).

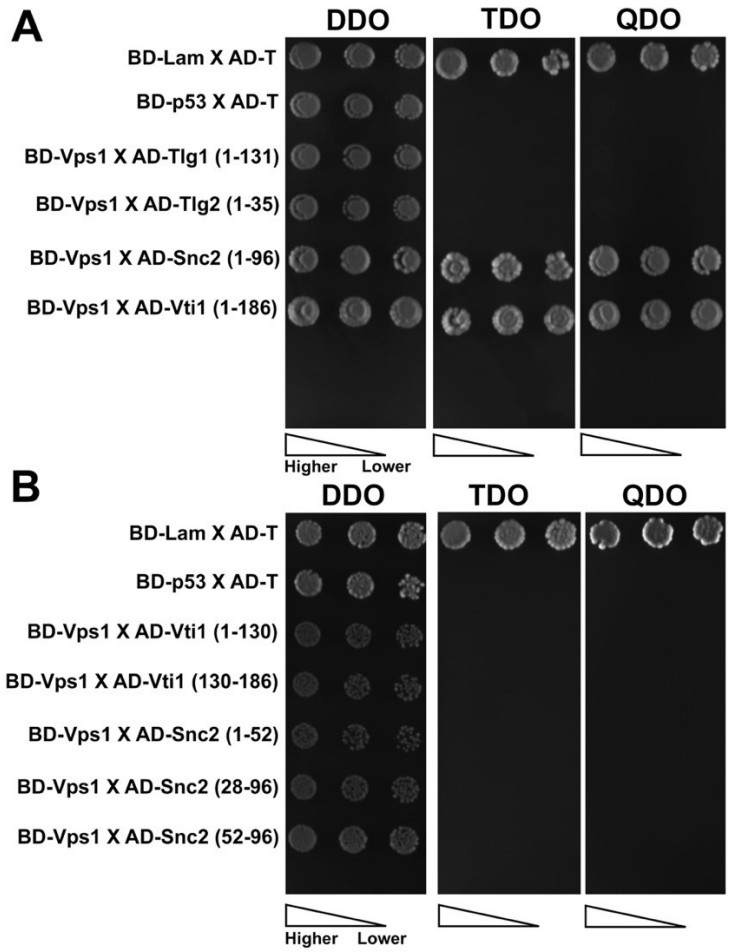

Figure 10. Interaction between Vps1 and cytosolic domains of Vti1 and Snc2 SNAREs. **A)** Vps1 physically interacts with N-terminally located cytosolic domains of Vti1 and Snc2. Diploid cells coexpressing BD-Vps1 and a cytosolic domain of a SNARE, Tlg1 (1-131 amino acid), Tlg2 (1-35 amino acid), Snc2 (1-96 amino acid) or Vti1 (1-186 amino acid) (KKY 1751, KKY 1727, KKY 1728, and KKY 1729 respectively) were spotted onto DDO, TDO, and QDO plates. The growth on DDO plates indicated that diploid cells were coexpressing both bait and the prey vector with the corresponding gene of interest. Cells coexpressing BD-Vps1 and AD-fused Snc2 (1-96 amino acid) or Vti1 (1-130 amino acid) showed growth on TDO and QDO plates, indicating the activation of two reporter genes, histidine, and adenine. However, diploid cells co-expressing BD-Vps1 and Tlg1 (1-131aa) or Tlg2 (1-35 amino acid) did not show growth on TDO or QDO plates. **B)** N-terminally located domains of Vti1 and Snc2 are necessary for the interaction with Vps1. Different N-terminal domains of Vti1 or Snc2 (Vti1 (1-130 amino acid), Vti1 (130-186 amino acid), Snc2 (1-52 amino acid), Snc2 (28-96 amino acid), and Snc2 (52-96 amino acid)) was fused to an AD vector and expressed in Y187 (KKY 1255) yeast cells. These strains were then coexpressed with BD-Vps1 in diploid cells (KKY 1868-1872 respectively). Spotting assay was performed.

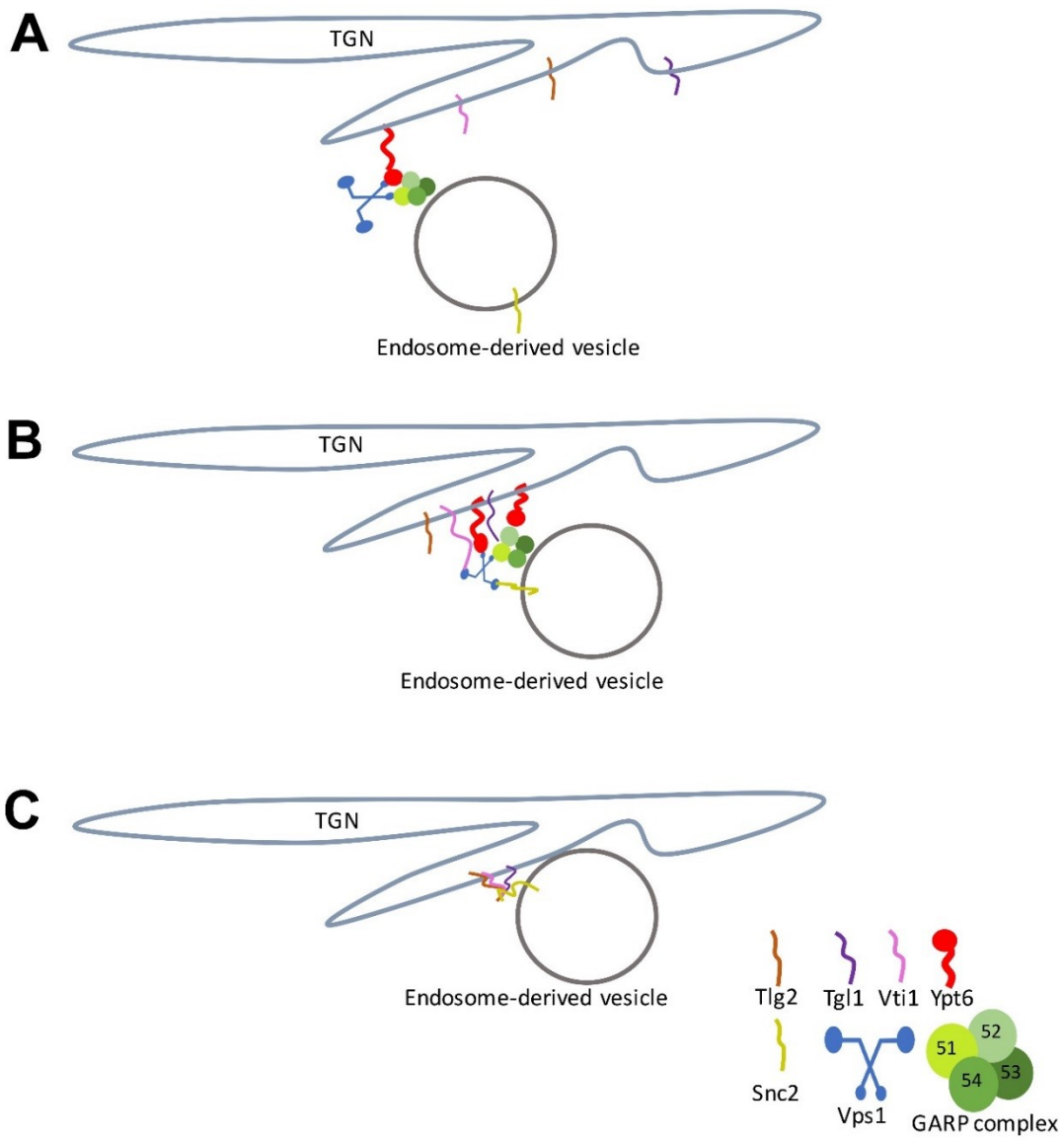

Figure 11. Ypt6 and Vps1 may cooperate to facilitate endosome-derived vesicle tethering and fusion at the TGN. **A)** Endosome-derived vesicle tethering at the TGN. Given that GTP-bound Ypt6 recruits the GARP complex to the TGN by interacting with Vps52 (Benjamin et al., 2011; Siniossoglou, 2005) and that Vps1 binds both to Vps51 (Saimani et al., 2017) and Ypt6 (Figure 3), it is likely that all these factors assemble into a multi-protein complex that strengthens the tethering of the vesicle to the TGN. **B)** Docking of the vesicle to the TGN. It was demonstrated that Vps51 interacts with Tlg1 so as to sturdily link the vesicle to the TGN (Siniossoglou and Pelham, 2002). Additionally, as a part of this multipartite protein complex, Vps1 probably acts as an adaptor-like protein that associates with Vti1 and Snc2 (Figure 10) to promote the formation of the 4-alpha-helix bundle. **C)** Fusion of the vesicle to the TGN. The 4-alpha-helix bundle of Tlg1, Tlg2, Vti1, and Snc2 forms a *trans*-SNARE complex (Parlati et al., 2002), leading to lipid mixtures of the vesicle and the TGN.